Aus der Klinik für Anästhesiologie
Anästhesie-, Intensiv-, Notfall- und Schmerzmedizin
(Direktor: Univ.- Prof. Dr. med. Klaus Hahnenkamp)
der Universitätsmedizin der Universität Greifswald

Potential Effects of Poloxamer 188 on Rat Isolated Brain Mitochondria after Simulated Ischemia/Reperfusion Injury

Inaugural - Dissertation

zur

Erlangung des akademischen

Grades

Doktor der Medizin
(Dr. med.)

der

Universitätsmedizin

der

Universität Greifswald

2022

vorgelegt von:
Johannes Aaron Pille
geb. am: 08.08.1997
in: Rom, Italien

Dekan: Prof. Dr. Karlhans Endlich

1. Gutachter: Prof. Dr. Klaus Hahnenkamp

2. Gutachter: Prof. Dr. Sebastian Haas

Ort, Raum: Seminarraum J 02.17 der Klinik für Orthopädie, Greifswald

Tag der Disputation: 20.10.2022

Table of Contents

List of Abbreviations

%	percent
°C	degree Celsius
$\Delta\psi_m$	mitochondrial membrane potential
µg	microgram
µl	microliter
µM	micromolar
µmol	micromole
10 min RT	10 minutes of exposure to room temperature
20 min RT	20 minutes of exposure to room temperature
ADP	adenosine diphosphate
ATP	adenosine triphosphate
BSA	bovine serum albumin
cf.	confer
Ca^{2+}	calcium
$CaCl_2$	calcium chloride
cmH_2O	centimeter of water
CT	computed tomography
CRC	calcium retention capacity
DAP	diadenosine pentaphosphate
ddH_2O	double-distilled water
DMSO	dimethyl sulfoxide
e^-	electron
EB	experimental buffer
ECG	electrocardiogram
EGTA	ethylene glycol-bis(2-aminoethylether)-N,N,N′,N′-tetraacetic acid
$FADH_2$	flavin adenine dinucleotide
FEP	fluorethylenpropylen
FiO_2	fraction of inspired oxygen
g	gravitational force
g	gram
h	hour
H^+	proton
H_2O_2	hydrogen peroxide

i.e.	id est
I/R	ischemia/reperfusion
IB	isolation buffer
in	inch
K_2HPO_4	potassium phosphate dibasic
KCl	potassium chloride
kg	kilogram
KH_2PO_4	potassium phosphate monobasic
KOH	potassium hydroxide
l	liter
LAD	left anterior descending coronary artery
M	molar
mg	milligram
min	minute
ml	milliliter
mm	millimeter
mM	millimolar
mmHg	millimeter of mercury
MPT	mitochondrial permeability transition
mPTP	mitochondrial permeability transition pore
mU	milliunit
N_2	nitrogen
Na^+	sodium
NADH	nicotinamide adenine dinucleotide
nm	nanometer
nM	nanomolar
O_2	oxygen
OGD	oxygen-glucose deprivation
P188	Poloxamer 188
PEO	polyoxyethylene oxide
PPO	polyoxypropylene oxide
RCI	respiratory control index
RLU	relative luminescence unit
ROS	reactive oxygen species

rpm	revolutions per minute
RT	room temperature
rtPA	recombinant tissue plasminogen activator
s	second
TBI	traumatic brain injury
TCA	tricarboxylic acid
U	unit
V	Volt
VUMC	Vanderbilt University Medical Center
W	Watt

List of Figures

List of Tables

1 Introduction

1.1 Clinical Background of Cerebral Ischemia

1.1.1 Epidemiology

Every year over 17 million strokes occur worldwide causing approximately 6 million people to die and over 100 million disability-adjusted life years to be lost, making cerebral ischemia one of the most fatal diseases in the world [1,2]. A similar impact of stroke can be observed in Germany, specifically, with a stroke incidence of approximately 270,000 per year and 53,119 people dying from cerebrovascular diseases in the year 2019 [3,4]. The high incidence of strokes has led to an implementation of so-called “stroke units” as specialized units for well-organized and timely diagnosis and treatment of strokes to which a good amount of hospital care capacity is dedicated [5]. Furthermore, post-acute care and rehabilitation are an additional significant part of stroke therapy from a medical as well as an economical perspective.

Traumatic brain injury (TBI) can cause local cerebral ischemia similar to a stroke and is suffered by approximately 1.4 million people per year in the US and 266,000 per year in Germany adding even more patients suffering ischemic brain injury [6,7].

Moreover, cerebral ischemia can not only occur locally during stroke or after TBI but also globally in the context of cardiac arrest. In fact, with over 17 million deaths every year, cardiac arrest is the most common cause of death in the world and this is mainly due to the brain injury that occurs during the arrest and after the return of spontaneous circulation [8,9]. In survivors of cardiac arrest, the sustained brain damage also continues to impede recovery [8].

Despite all efforts, many surviving patients continue to suffer permanent disabilities [1,8], and all these grave circumstances surrounding stroke and cerebral ischemia in general emphasize the critical need for better prevention, diagnostics and especially therapy [10].

1.1.2 Etiology

Cerebral ischemia can occur through multiple ways, the most common being ischemic stroke [1]. An ischemic stroke results from the sudden occlusion of a cerebral vessel, which cannot always be retraced to a specific cause, and the subsequent focal ischemia [10,11]. On the basis of its pathology, ischemic strokes are mainly

categorized into cardio-embolic (i.e. from atrial fibrillation), large artery athero-thrombotic, and lacunar stroke [10].

Non-traumatic cerebral hemorrhage occurs through the rupture of a cerebral blood vessel and subsequent intracranial bleeding leading to a hemorrhagic stroke [11]. Cerebral hemorrhage causes increased intracranial pressure and local compression of surrounding structures and only the former can lead to ischemia [12]. By definition a hemorrhagic stroke occurs only with non-traumatic cerebral hemorrhage; if caused by trauma cerebral hemorrhage would be assigned to TBI [11].

TBI is generally caused by blunt trauma to the head which leads to reduced cerebral perfusion and subsequent ischemia [7]. While in the US motor vehicle crashes are the primary reason for TBI, in Germany falls are a much more common cause [7,13].

Cardiac arrest, in turn, can have a multitude of reasons, among others coronary artery disease, cardiomyopathy, or myocarditis [14]. Independently of the cause, cardiac arrest leads to an abrupt stagnation of cerebral blood flow causing cerebral ischemia [15].

1.1.3 Diagnostics and Therapy

Depending on the localization of the ischemia in the brain, a variety of symptoms can emerge. The most prominent are sudden unilateral weakness, numbness, or visual loss, caused by ischemic injury in any of the six bilaterally arranged cerebral arteries or their branches [2,16]. However, when ischemia occurs in the cerebellum, symptoms like ataxia, nausea, vertigo or even just dizziness become prevalent [16].

When a stroke is suspected, the patient should undergo emergency non-contrast cranial computed tomography (CT) or magnetic resonance imaging. While a hemorrhagic stroke is easy to diagnose or visualize by CT, the ischemic stroke might be more difficult to detect depending on the size, localization or point in time since vessel occlusion [2].

Within the first 4.5 h of ischemic stroke after diagnosis, patients should receive 0.9 mg kg^{-1} intravenous alteplase (recombinant tissue plasminogen activator: rtPA), which has been shown to significantly improve clinical outcome [17]. This improvement increases even further, the earlier the alteplase is administered [2].

Although the ideal circumstances for successful use still have to be investigated, endovascular thrombectomy is increasingly being performed and has been included in the American as well as the European guidelines [2,18,19].

In contrast, a hemorrhagic stroke as well as TBI may require surgical treatment, the extent of the latter depending on hematoma site, diameter, and volume [2,7].
The treatment of cardiac arrest must be adapted to the underlying cause but primarily consists of cardiopulmonary resuscitation and, in case of a shockable rhythm, defibrillation [20–24].
In the long term, recovery and rehabilitation is the main subject for patients who suffered cerebral ischemia, since many show various forms and degrees of disabilities. Each patient, therefore, needs an adapted rehabilitation program suitable to improve his/her capabilities [2].

1.2 Theoretical Background: Biochemistry of Mitochondria

Mitochondria as the so-called powerhouses of the cell are the cell organelles in which the tricarboxylic acid (TCA) cycle and oxidative phosphorylation take place and are therefore responsible for adenosine triphosphate (ATP) synthesis [25,26]. However, they are involved in a multitude of other intra- and intercellular processes all of which can cause a multitude of different diseases when negatively affected [27].
Mitochondria play an especially vital role in ischemic processes since the lack of oxygen (O_2) causes the mitochondria to stop producing ATP and to trigger multiple apoptotic pathways [28]. To investigate the implications of ischemia in cells and especially in mitochondria it is crucial to understand the different underlying functions of the latter.

1.2.1 Mitochondrial Membrane

Similar to cells, mitochondria have a membrane of their own. However, instead of consisting of one phospholipid bilayer, the mitochondrial membrane is made of an outer and inner membrane each composed of a phospholipid bilayer (Figure 1). The outer membrane's constitution is similar to the cell membrane and is permeable to small molecules like electrolytes and metabolites [29]. This causes the intermembrane space between the outer and inner mitochondrial membranes to have the same concentrations of these small molecules as in the cytosol [29]. Bigger proteins, however, need specific signaling peptides that are recognized and enable these proteins to be transported into the intermembrane space [30].
The inner membrane is less permeable than the outer and is folded in itself to create cristae [29]. It contains the respiratory chain enabling mitochondria to create a

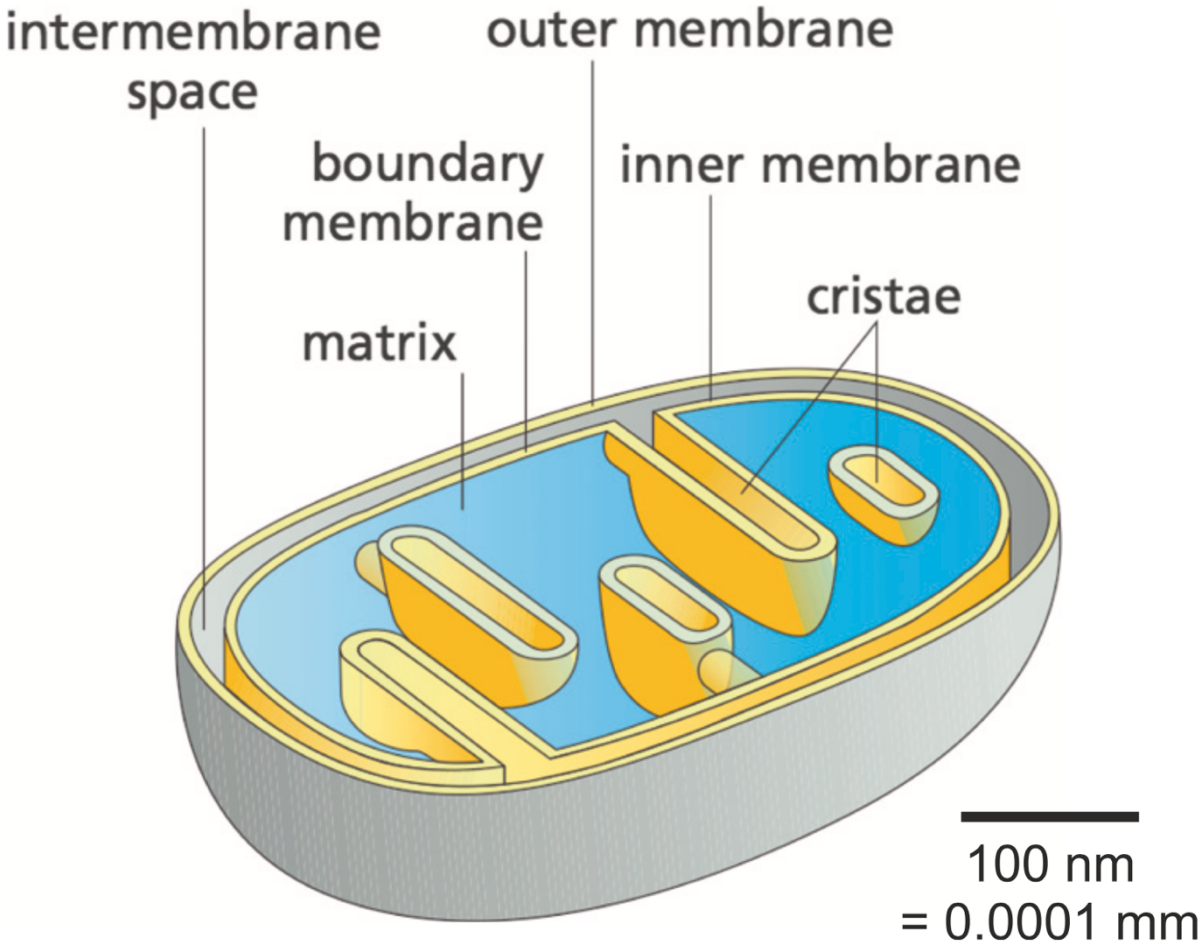

Figure 1: Mitochondrial Membrane Compartments
The outer membrane confines the intermembrane space and the inner membrane mitochondrial matrix. The inner membrane also creates cristae by folding itself into the matrix and thereby increases the surface for adenosine triphosphate production. According to Kühlbrandt, 2015 [33]

chemical proton gradient and the mitochondrial membrane potential ($\Delta\psi_m$) which in turn fuel the ATP production [31,32].

1.2.2 Respiratory Chain

The respiratory chain's main function is to transport protons (H^+) from the mitochondrial matrix into the intermembrane space by oxidation of electron (e^-) donors and reduction of e^- acceptors [25,31]. While the e^- donors are produced in the TCA cycle and in the β-oxidation, the acceptors are located in the inner mitochondrial membrane in form of the complexes I to IV [25,29]. Up to ten H^+ molecules can be transported into the intermembrane space by transporting e^- coming from reduced nicotinamide adenine dinucleotide (NADH) or flavin adenine dinucleotide ($FADH_2$) through these complexes [34].

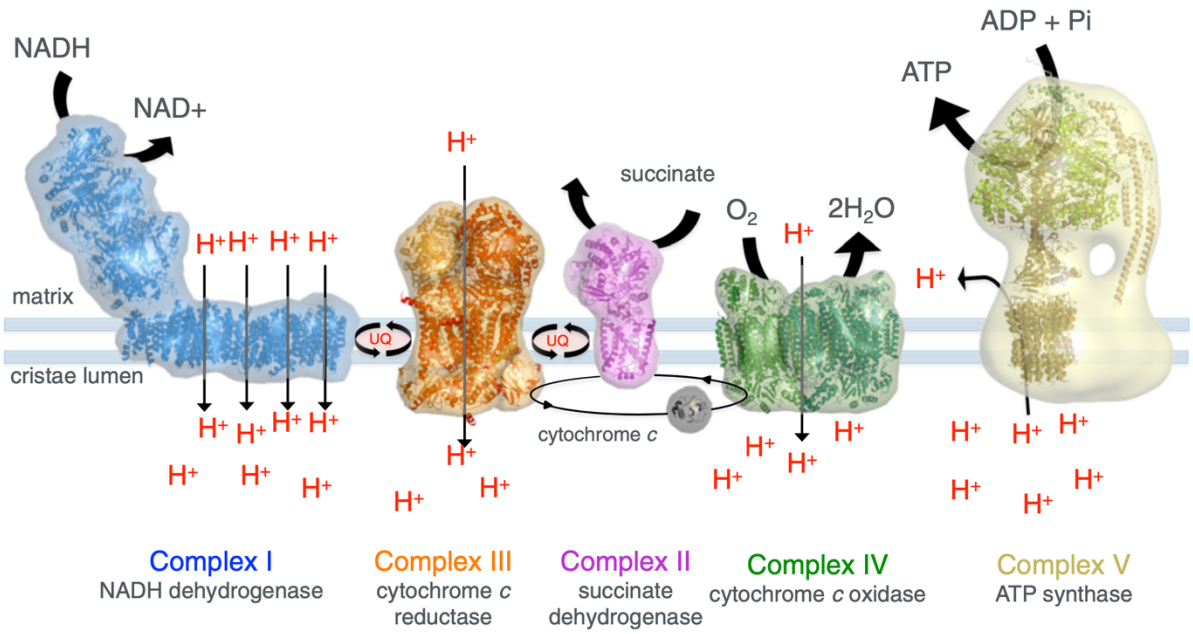

Figure 2: Mitochondrial Respiratory Chain
Through oxidation of electron (e^-) donors and reduction of e^- acceptors proton (H^+) molecules are transported through the inner mitochondrial membrane, creating an H^+ gradient. This gradient, in turn, fuels the adenosine triphosphate (ATP) synthase to produce ATP. According to Kühlbrandt, 2015 [33]

While complex I and II accept e^- from NADH and $FADH_2$, respectively, complex III and IV only transfer e^- passed on by complexes I and II [29]. In complex IV, the e^- are added to an O_2 atom together with two H^+ to then form water (Figure 2) [29].
At last, the electrochemical gradient built up by transferring H^+ into the intermembrane space can now fuel the ATP synthase to produce ATP from adenosine diphosphate (ADP) and inorganic phosphate [29].

1.3 Ischemia/Reperfusion Injury

An ischemic process severely damages surrounding tissue and will eventually lead to tissue death, making reperfusion as soon as possible the pivotal treatment [35]. However, reperfusion is known to inflict additional damage that may be even greater than the ischemic damage itself [35,36]. The underlying processes of both the ischemic as well as the reperfusion injury have to be elucidated in order to understand the complexity of ischemia/reperfusion (I/R) injury.

1.3.1 Biochemical Reactions

During ischemia the lack of O_2 causes the cells' metabolism to change to anaerobic glycolysis [35]. Lactate accumulates in the cell leading to a decreased pH [35]. This, in turn, triggers the activation of the sodium (Na^+)-H^+ exchanger to pump out the H^+ in

exchange for Na^+ [35]. The extended anaerobic metabolism is not able to sustain the normal intracellular ATP levels, and the lack of ATP inactivates the ATPases [35]. Due to this inactivity, calcium (Ca^{2+}) ions can no longer be transported out of the cytoplasm and accumulate [35]. The Ca^{2+} overload can, furthermore, cause activation of mitochondrial permeability transition pores (mPTPs) [37,38]. The resulting mitochondrial permeability transition (MPT) further impairs ATP production [35].

While reperfusion is crucial for tissue restoration, the reintroduction of oxygenated and substrate-rich blood into the damaged tissue can – as mentioned above – wreak further damage [35]. The Ca^{2+} overload that already occurs during ischemia further intensifies causing an increasingly potent MPT [35]. The reintroduced O_2 provokes the production of reactive oxygen species (ROS) which do not only further damage the cells but also trigger a pro-inflammatory response [35]. If necrosis has not occurred yet, the ROS, the inflammatory response, the Ca^{2+} overload, and the MPT will cause the induction of apoptosis (Figure 3) [35,36].

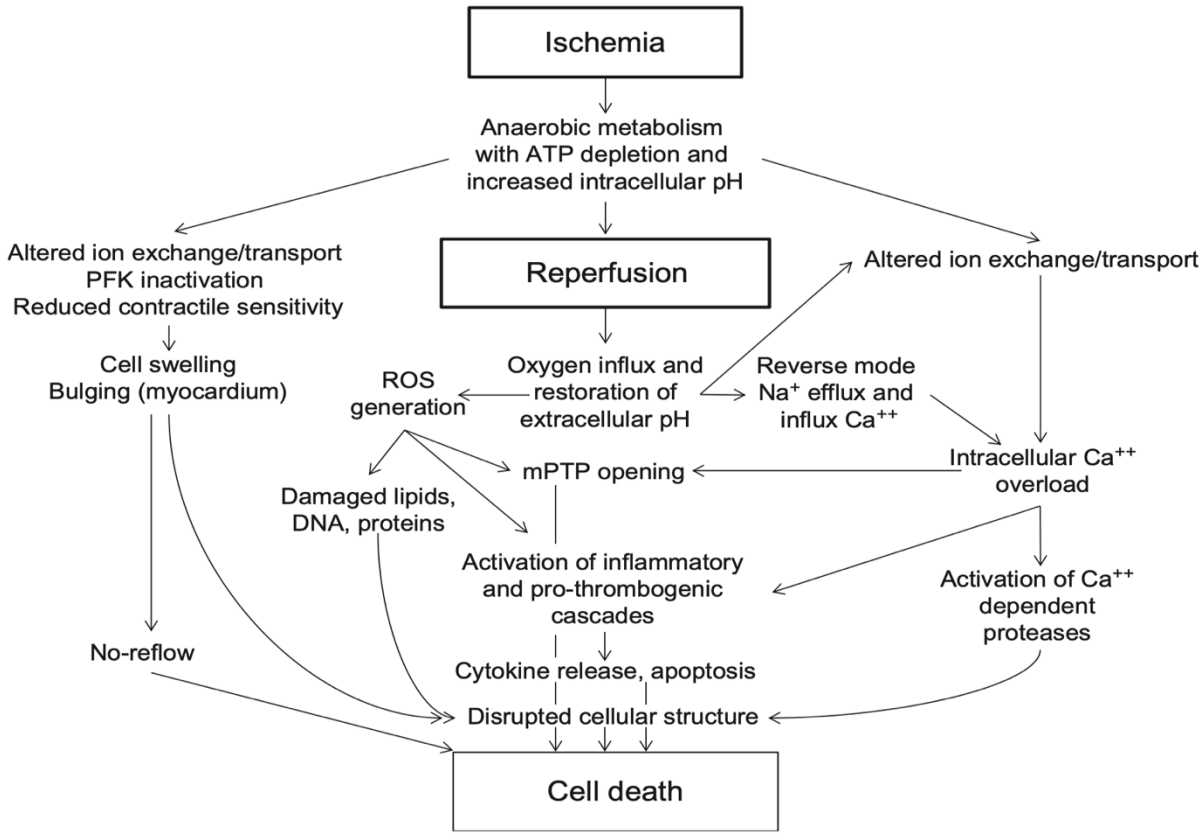

Figure 3: Pathological Chain Reaction during I/R Injury
While ischemia causes the primary injury, reperfusion induces additional detrimental damage to the cell. According to Kalogeris et al., 2012 [35]

1.3.2 Effects on Mitochondrial Metabolism

The important role of mitochondria in this context of I/R injury is the subject of increasing research [35]. While mitochondria are negatively affected during I/R, they also contribute to the deteriorating intra- and extracellular reactions [37].

With the lack of O_2, the respiratory chain will be inhibited, and the $\Delta\psi_m$ begins to collapse [35]. Not only are the mitochondria not able to synthesize ATP anymore. To sustain the $\Delta\psi_m$, the ATP synthase will even start running in reverse mode through hydrolyzation of ATP, further decreasing the cellular ATP levels [35].

Without oxidative phosphorylation, the TCA cycle and the β-oxidation will be impeded as well [35]. Toxic fatty acids with pro-inflammatory properties accumulate [35].

Inhibition of the respiratory chain also causes production of ROS in multiple ways [35,37]. For instance, complexes I and III will remain in a reduced state catalyzing the production of ROS [35]. The cell's antioxidant system tries to buffer these but becomes quickly overwhelmed [35].

Formation and opening of the mPTP are a critical event during I/R injury [35]. MPT is triggered by many circumstances described above and amplifies already existing issues [35]. During ischemia, low pH prevents MPT. However, rising cytoplasmatic Ca^{2+} concentrations, production of ROS, and accumulating toxic fatty acids eventually open the mPTP [35]. This causes a complete collapse of the $\Delta\psi_m$ as H^+ easily passes through the mPTP into the matrix [35,39]. This transition of H^+ pulls water following the osmotic gradient into the mitochondrial matrix which causes mitochondrial swelling and possibly even rupturing [35,39].

1.4 Poloxamer 188

Poloxamer (P)188 is a triblock copolymer used in cosmetic, industrial as well as pharmaceutical applications [40,41]. P188 has been a focus of research since the 1980's in regard to its various biological effects [40]. Specific to I/R injury, findings indicate that P188 is able to significantly improve resealing of damaged cell membranes [40,41].

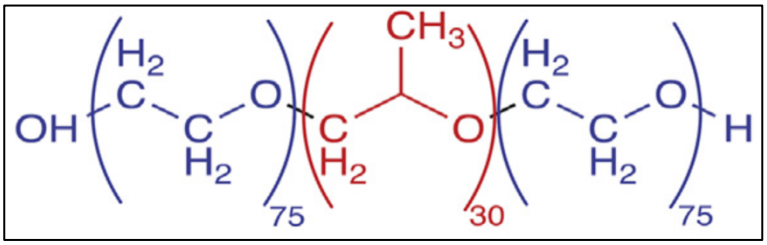

Figure 4: Structural Formula of Poloxamer 188
Poloxamer 188 consists of two hydrophilic polyoxyethylene oxide chains (blue) connected through a hydrophobic polyoxypropylene oxide chain (red). According to Houang et al., 2019 [41]

1.4.1 Chemical Properties and Principle of Biological Effects

As a nonionic triblock copolymer, P188 consists of a central hydrophobic chain of polyoxypropylene oxide (PPO) and two hydrophilic chains of polyoxyethylene oxide (PEO) on each side (Figure 4) [40,41]. This composition makes P188 a molecule with an amphiphilic character [40].

Different mechanisms of protection are proposed for P188, however, the principal idea behind its membrane-sealing effect is that during membrane damage and poration the hydrophobic component of P188 will interact with the membrane pores and physically seal it (Figure 5) [41–43].

1.4.2 Various Biomedical Applications

While the present study focusses primarily on its effects during I/R injury, P188 has in fact been first examined as an anti-viscosity agent and as such has even been

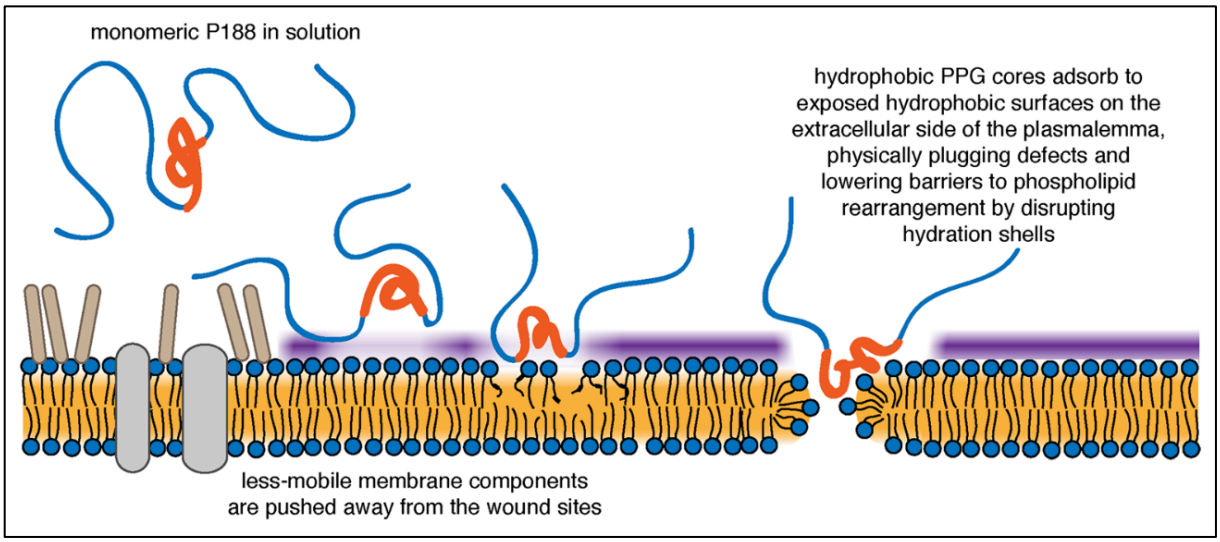

Figure 5: Principle of Membrane Stabilization by Poloxamer 188
The hydrophobic polyoxypropylene oxide [PPO (=PPG]) is thought to interact with the exposed hydrophobic part of the damaged phospholipid bilayer. According to Poellmann and Lee, 2017 [42]

approved by the US Food and Drug Administration in sickle cell anemia [41,44]. Its ability to alter the rheologic properties of the blood has been used to not only lessen blood viscosity but also platelet aggregation [41,44]. P188 has also been reported to enhance blood oxygenation, and other poloxamers have been applied as drug delivery adjuvants [44].

Extensive effort, however, has been put into studying P188's membrane stabilization capabilities [40,41]. Duchenne muscular dystrophy as a muscle membrane pathology is exemplary for an application of P188 [41,44]. Due to a lack of dystrophin the cell membrane is not linked to the actin cytoskeleton making it unstable [44]. The amphiphilic properties of P188, in turn, allow stabilization of the damaged muscle membrane. Membrane damage and instability also occurs in various tissues during I/R making the possible application of P188 in settings like myocardial infarction, ischemic stroke, or cardiac arrest a topic of interest [41–43,45].

1.4.3 Effect on Myocardial Cells during Ischemia/Reperfusion

Animal studies have shown that P188 significantly reduces infarct size after induced myocardial infarction [46]. A phase II clinical trial in 1997 did not show any significant effects for P188 when given to patients receiving thrombolytics for ST segment elevation myocardial infarction [47]. However, the analysis of the study protocol showed that the interval between application of thrombolytics and the infusion of P188 varied up to 30 min [45]. This issue led Bartos et al. to reconsider P188 as a possible treatment for I/R injury in the context of myocardial infarction, this time focusing on immediate intracoronary application of P188 upon reperfusion and comparing this approach to a delayed intravenous application – similar to the one used in the previously described clinical trial – in a porcine model [45]. This latest study has not only shown the reduction of infarct size that had already been pointed out in older studies [45]. Bartos et al. also isolated heart mitochondria in this context and found significantly improved mitochondrial function in those pigs that were treated with P188 upon reperfusion [45].

1.4.4 Effect on Brain Cells

Discussing I/R injury in neurons, pathologies like ischemic stroke, TBI, or cardiac arrest would primarily come to mind. Some research, however, has branched out into non-I/R associated pathologies showing neuroprotection in models of intracranial hemorrhage or even in a mouse model of Parkinson's disease [41,42,48,48], Yet,

cerebral ischemia and TBI are the main focus when it comes to neuroprotective effects of P188 [41,42,49–61].

Early studies tried to attribute the neuroprotective effects to rheological properties since amongst other things it was shown that P188 improved blood flow to ischemic areas after occlusion of the middle cerebral artery in rabbits [41,42,61]. However, this has been contradicted as newer research hinted to the membrane stabilization capability of P188 [41,42]. In fact, P188 is able to preserve membrane integrity and hereby prevent neuronal death during simulated I/R in vitro in form of oxygen-glucose deprivation (OGD) [49]. Similar to cardiomyocytes, brain cells also show improved mitochondrial function after simulated I/R injury when treated with P188 [55]. P188 has been shown to be effective in TBI as well: P188 seems to prevent blood brain barrier damage and inhibit diffuse axonal injury by preventing axonal beading after simulated TBI [41,50] Additionally, in a model of in vitro TBI, it was able to attenuate mitochondrial and lysosomal membrane permeabilization [56]. P188 has also been shown to be neuroprotective against excitotoxicity, oxidative stress, as well as lipid peroxidation and decreases activation of autophagy after OGD [41,43].

Neuroprotection by P188 proves to be relevant from a clinical perspective, too, as it has exhibited reduced infarct volume and neurological deficits as well as improved long-term recovery in in vivo models of I/R injury [41].

1.5 Aims of the Study

Cerebral ischemia continues to affect many patients dramatically every year, even though newer and better therapies are constantly being developed. [1,2,18,19]. Through research on the multiple components of ischemic injury, the return of blood flow (i.e. reperfusion) – while absolutely necessary – has been determined as a strong contributing factor to cell death leading to the term of ischemia/reperfusion (I/R) injury [35,36]. Interestingly, mitochondria seem to play a crucial role in I/R injury making them a target for potential therapies [35,37,39].

After having determined the effectiveness of the triblock copolymer P188 on different cell types based on the cell-membrane-sealing effect shown in several studies [41,43–46,49,50,55,56,62], the highly significant effect on mitochondrial function parameters remained intriguing [45,62]. The protective influence on cell membranes with the subsequent cellular recovery could just generally lead to better preserved mitochondrial function as a consequence. However, mitochondria are encapsulated not only by one but two biolipid membranes with those being severely damaged during I/R injury as well.

Therefore, we hypothesized that P188 might have a direct sealing effect on the mitochondrial membranes and subsequently preserve their function. To determine if there is a direct influence of P188 on mitochondrial membranes after I/R injury our experiments aimed at:

a) Development of a model of I/R injury in rat isolated forebrain mitochondria through the in vitro addition of the ROS hydrogen peroxide (H_2O_2) as a component of I/R injury
b) Development of a model of I/R injury through in vivo asphyxial cardiac arrest in rats before isolation of forebrain mitochondria
c) Determination of a potential positive effect of P188 on isolated, injured mitochondria through assessment of ATP synthesis, O_2 consumption, and calcium retention capacity (CRC)

Positively increased mitochondrial function would show that a direct effect of P188 on mitochondria should be taken into consideration when trying to explain the positive effects of P188 in I/R injury.

2 Materials and Methods

All experiments were conducted in the Riess Lab of the Vanderbilt University Medical Center (VUMC), Nashville, TN, USA.

2.1 Materials

Table 1: Equipment

Name	*Company*	*Catalog No.*
-20°C Freezer	Frigidaire	FFU17FHW4
10 mL LL Syringe	B. Braun Medical Inc.	4617100V-02
10 µL Microliter Syringe Model 701 N, Cemented Needle, 22s gauge, 2 in., point style 3	Hamilton Company	80365
4°C Refrigerator	Frigidaire	FFU17G4JW25
5 µL Microliter Syringe Model 75 N, Cemented Needle, 26s gauge, 2 in, point style 3	Hamilton Company	87919
Avanti® J-E Centrifuge	Beckman Coulter, Inc.	369001
Corning™ Sterile Spatulas, Round end	Fisher Scientific	14-245-97
DWK Life Sciences Potter-Elvehjem Tissue Grinders, PTFE Pestle and Unground Glass Tube	Fisher Scientific	K886000-0024
FelixG software	Photon Technology International	Version 4.2.2.5265
Fluorescence Spectrophotometer	Photon Technology International	custom
Friedman Rongeur	Fine Science Tools	16000-14
GloMax® 20/20 Luminometer	Promega Corporation	E5311

Hardened Fine Scissors	Fine Science Tools	14090-09
LabChart	ADInstruments Inc.	Version 8.1.16
Mainstream etCO_2 sensor - Novametrix Cap 3	Koninklijke Philips N.V.	ACO2
Mitocell Respirometry System	Strathkelvin Instruments Ltd.	MS200A; MT200A; SI130; SI021
PERIFIX Catheter Connector	B. Braun Medical Inc.	332283
pH 700 Benchtop Meter	OAKTON Instruments	WD-35419-03
Polyamide/Polyurethane PERIFIX ONE Catheter	B. Braun Medical Inc.	333541
PowerLab 16/30	ADInstruments Inc.	ML880
Programmable Microfluidics Syringe Pump	Braintree Scientific, Inc.	BS-800 2X
Quartz SUPRASIL Fluorescence Cells for Magnetic Stirrers, 4 mm, 500 µL	PerkinElmer Inc.	B0631132
Rainin Classic Pipette (Various Volume Increments; Single- and Multi-Channel)	METTLER TOLEDO	17008708
Rodent Guillotine	World Precision Instruments	DCAP
Small Animal Ventilator (Model 683), Single Animal, Volume Controlled	Harvard Apparatus	55-0000
Synergy H1 Hybrid Multi-Mode Reader	BioTek Instruments, Inc.	H1MF
Tuohy Needle	B. Braun Medical Inc.	332166
UltraRocker Rocking Platform	Bio-Rad Laboratories, Inc.	1660719

Table 2: Chemical Substances, Reagents, Solutions, Kits

Name	*Company*	*Catalog No.*
Adenosine 5'-triphosphate	Thermo Fisher	A22066
Adenosine 5′-diphosphate monopotassium salt dihydrate	Sigma-Aldrich	A5285
Bio-Rad Protein Assay Dye Reagent Concentrate	Bio-Rad Laboratories, Inc.	5000006
Bovine Serum Albumin	Fisher Scientific	BP1600
Calcium chloride dihydrate	Sigma-Aldrich	C3881
Calcium Green™-5N, Hexapotassium Salt, cell impermeant	Thermo Fisher	C3737
D-Luciferin sodium salt	Tocris	5427
D-Mannitol	Sigma-Aldrich	M4125
Dimethyl sulfoxide	Sigma-Aldrich	D5879
Ethylene glycol-bis(2-aminoethylether)-N,N,N′,N′-tetraacetic acid	Sigma-Aldrich	E4378
Heparin Sodium Injection, USP	West-Ward Pharmaceuticals	0641-2450-55
Hydrogen peroxide solution	Sigma-Aldrich	216763
KetaVed® Ketamine Hydrochloride Injection, USP	Vedco Inc.	50989-996-06
Kolliphor® P 188	Sigma-Aldrich	15759
L-(−)-Malic acid disodium salt	Sigma-Aldrich	M9138
L-Glutamic acid monosodium salt hydrate	Sigma-Aldrich	G1626
Luciferase	G-Biosciences	786-1309
MOPS	Sigma-Aldrich	M3183
P^1,P^5-Di(adenosine-5′) pentaphosphate pentasodium salt	Sigma-Aldrich	D4022
Pentobarbital	Diamondback Drugs	G2270-0235-50
Percoll®	Cytiva	17-0891-01
Potassium chloride	Sigma-Aldrich	P4504

Potassium hydroxide	Sigma-Aldrich	P1767
Potassium phosphate dibasic trihydrate	Sigma-Aldrich	P5504
Potassium phosphate monobasic	Sigma-Aldrich	P5379
Rocuronium bromide	Pfizer Inc.	NDC 0409-9558-05
Rotenone	Sigma-Aldrich	R8875
Sodium succinate dibasic hexahydrate	Sigma-Aldrich	S2378
Sucrose	Sigma-Aldrich	S7903

Table 3: Expendables

Name	*Company*	*Catalog No.*
Absorbent Underpads with Waterproof Moisture Barrier	VWR International, LLC	82020-845
Corning® Costar® microcentrifuge tubes with snap cap	Sigma-Aldrich	CLS3213
Disposable Graduated Transfer Pipettes	Fisher Scientific	13-711-9AM
Fiber C-Fold Towels	Fisher Scientific	19-120-2484
Hexagonal Polystyrene Weighing Dishes	Fisher Scientific	02-202-100
High-Speed Round-Bottom PPCO Centrifuge Tubes	Fisher Scientific	05-562-10K
Light Sensitive Centrifuge Tube 50 ml	VWR International, LLC	10026-094
Light-Duty Tissue Wipers	VWR International, LLC	82003-822
Microcentrifuge tubes with attached lid	Sigma-Aldrich	T6649
Polystyrene Weighing Boats	Fisher Scientific	13-735-744
Reagent Reservoir Basins	RPI	246282
Thermo Scientific™ Nunc™ MicroWell™ 96-Well Microplates	Fisher Scientific	12-565-226

2.2 Buffers

2.2.1 Isolation Buffer

Table 4: Chemical Ingredients for Isolation Buffer

Concentration	*Chemical*	*Amount per liter*
200 mM	Mannitol	36.4 g l^{-1}
50 mM	Sucrose	17.1 g l^{-1}
5 mM	KH_2PO_4	0.68 g l^{-1}
5 mM	MOPS	1.05 g l^{-1}
0.1%	BSA	1 g l^{-1}
1 mM	EGTA	0.38 g l^{-1}

The isolation buffer (IB) used in all steps of mitochondria isolation was stored at 4°C and made fresh every 2 weeks. Typically, 1 l of buffer was prepared and was sufficient till the expiration of 2 weeks.

Mannitol was dissolved in a beaker with ~900 ml double-distilled water (ddH_2O) and heated for 1 h while stirring. Thereafter, it was left to cool down to room temperature (RT). The remaining components were added and the beaker was filled up to almost one liter leaving enough volume for the pH adjustment. Finally, the pH was adjusted to 7.15 using 8 M potassium hydroxide (KOH) solution while consistently measuring the pH with the Oakton® pH 700 Benchtop pH Meter and the beaker definitively filled up to one liter; it should be noted that the ethylene glycol-bis(2-aminoethylether)-N,N,N′,N′-tetraacetic acid (EGTA) would not dissolve before the pH adjustment.

2.2.2 Percoll Solutions

The 40%, 24% and 15% Percoll solutions were made up in IB. They were stored at 4°C and made fresh every 2 weeks.

2.2.3 Experimental Buffer

The experimental buffer (EB), which was used in the mitochondrial function assays, was stored at 4°C and made fresh every 2 weeks, just like the IB.

The ingredients were added into 1 l of ddH_2O and the pH adjusted to 7.15 with 8 M KOH solution.

Table 5: Chemical Ingredients for Experimental Buffer

Concentration	*Chemical*	*Amount per liter*
130 mM	KCl	9.7 g l^{-1}
5 mM	K_2HPO_4	1.14 g l^{-1}
20 mM	MOPS	4.18 g l^{-1}
0.1%	BSA	1 g l^{-1}

2.2.4 No-Phosphate Experimental Buffer

In addition, an EB without phosphate was needed for the CRC assay, which was made in the same way as the EB excluding potassium phosphate dibasic (K_2HPO_4). It was stored at 4°C and made fresh every 2 weeks. Usually, not more than 250 ml of no-phosphate EB were needed for this timespan.

2.2.5 Substrates for Mitochondrial Function Assays

Table 6: Substrate Concentrations for Different Assays

	Complex I activation	*Complex II activation*
ATP synthesis assay	1 M glutamate in EB; 1 M malate in EB	0.5 M succinate in EB; 0.5 mM rotenone in DMSO
Oxygen consumption & calcium retention capacity assay	2 M glutamate in EB; 2 M malate in EB	1 M succinate in EB; 1 mM rotenone in DMSO

Aliquots of 100 µl were prepared for all substrates, stored at -20°C and made fresh every 2 weeks, except for the rotenone solutions which were useable for an unlimited period of time.

On experiment day the glutamate and malate were combined to result in a 0.5 M glutamate/0.5 M malate solution for the ATP synthesis assay and a 1 M/1 M solution, respectively, for O_2 consumption and CRC assays.

2.2.6 Assay Buffers

To facilitate the preparation of ATP synthesis assay buffer on experiment days, 100 µl aliquots of 20 µM diadenosine pentaphosphate (DAP) and 3 mM ADP were made before and stored at -20°C.

Table 7: Chemical Ingredients for ATP Synthesis Assay Buffer

0.2 µM	DAP
30 µM	ADP
0.1 mg ml^{-1}	luciferin
1.25 µg ml^{-1}	luciferase

100 µl aliquots were also made of 25 mM ADP, used for the O_2 consumption assay.
For the CRC assay a 10 mM calcium chloride ($CaCl_2$) solution was prepared in no phosphate EB every 2 weeks and stored at -20°C.
Furthermore, a main stock of 1 mM Calcium Green solution was prepared in dimethyl sulfoxide (DMSO) and stored at -20°C for an unlimited period of time. Then, a secondary stock of 10 µM Calcium Green was prepared in EB every 2 weeks and stored at -20°C. On the day of the experiment, a 100 nM Calcium Green EB was prepared for immediate use.

2.3 Laboratory Animals

The animals used were male Sprague-Dawley rats (350-450 g). Their use had been authorized by the Institutional Animal Care and Use Committee of the VUMC. Rats undergoing immediate euthanization were used only from the protocols M1600012 and M1700168. Rats in which asphyxial cardiac arrest was induced were handled only by authorized personnel until euthanasia and belonged to the protocol M1800029.

2.4 Animal Preparation

2.4.1 Animal Preparation before Euthanasia for In Vitro Injury

Thirty-four rats were anesthetized with intraperitoneal administration of 100 mg ketamine per kg bodyweight. If the amount of ketamine was not enough to sedate the animal after 15 min a supplementary dose of 5 mg kg^{-1} ketamine would be administered. Supplementary doses were given every 10 min until the animal would not show any reaction to tail and toe pinch. 5 min before euthanasia by decapitation (cf. 2.4.3 Euthanization and Brain Extraction), 3,000 U Heparin per kg bodyweight were administered.

2.4.2 Animal Preparation for In Vivo Asphyxial Cardiac Arrest

To prepare for asphyxial cardiac arrest, 9 rats were anesthetized with intraperitoneal administration of 50 mg pentobarbital per kg bodyweight. Supplementary doses with 10 mg kg^{-1} were given if needed until the animal was nonreactive to pain stimuli. Following a protocol modified from Lamoreux et al. [63], the animals were intubated; vascular access was achieved via cannulation of the tail vein and surgical cutdown of femoral vein and artery. Electrocardiogram (ECG) via subcutaneous ECG needles, rectal temperature, arterial blood pressure, and venous waveforms were recorded using PowerLab and LabChart.

Using an animal ventilator, rats were ventilated with a tidal volume of 0.6 ml kg^{-1}, FiO_2 0.25, positive end-expiratory pressure of 5 cmH_2O, and a respiratory rate adjusted to achieve an endtidal CO_2 of 40 ± 5 mmHg, measured by an infrared CO_2 sensor. Rats were then randomized into cardiac arrest vs. a sham procedure (cf. 2.7.2 In Vivo by Asphyxial Cardiac Arrest).

2.4.3 Euthanization and Brain Extraction

After proper sedation, the animal was decapitated with the guillotine. The skull was cut open with scissors starting from the occipital bone and continuing to splice up the suture between the parietal bones. The parietal bones were flapped out to the sides with a rongeur, and the brain became accessible. After removing the cerebellum with a spatula, the forebrain was scooped out and placed into ~10 ml cold IB.

2.5 Isolation of Mitochondria

The brain mitochondria were isolated following – with some modifications by the Riess Lab – the procedure of Tibor Kristian [64] using differential centrifugation. The buffers used are mentioned above and derive from [65]. Throughout the isolation process the IB used was always kept on ice to keep it at the right temperature.

After placing the brain in IB, the tissue was rinsed clear of blood by adding more IB and pipetting the IB up and down with a plastic pipette. After weighing the brain in a weighing boat – and subtracting any remaining fluid weight in the boat after taking out the brain –, it was placed in a beaker with ~3 ml IB. Using scissors the tissue was minced into ~1 mm pieces and transferred to a homogenizing vessel. ~10 ml of IB were added and the pestle was passed up and down 8 to 10 times in the homogenizer until the homogenate was smooth and uniform. The homogenate was transferred into a

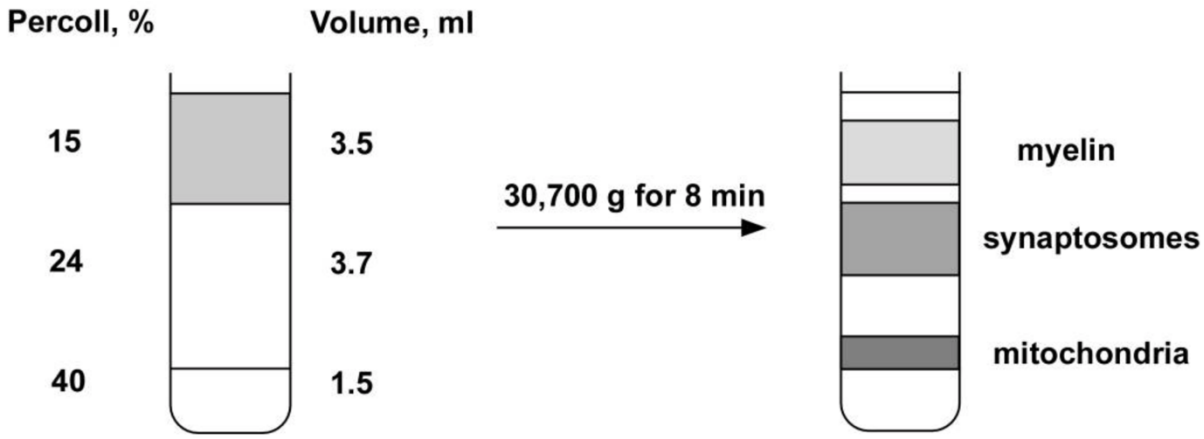

Figure 6: Percoll Gradient and Distribution of Brain Homogenate Fractions
The Percoll gradient consists of three layers of different Percoll ratios. The brain homogenate distributes into three fractions during centrifugation. According to Kristian, 2010 [64]

50 ml centrifuge tube and centrifuged (1,300 *g* at 4°C for 3 min). The supernatant was carefully transferred into a new tube placed on ice. The pellet was gently dislodged and homogenized in ~5 ml of IB with a plastic transfer pipette. The new homogenate was centrifuged again at 1,300 *g* at 4°C for 3 min. The resulting supernatant was combined with the supernatant collected from the first centrifugation. The pooled supernatants were centrifuged at 21,000 *g* at 4°C for 10 min. In the meantime, the Percoll gradient (Figure 6) was prepared as follows [64]:

7.4 ml of 24% Percoll were added into a centrifugation tube. To ensure a more careful insertion of the next layer 3 ml 40% Percoll were first added into a separate tube with a volumetric pipette. The 3 ml of 40% Percoll were collected with a transfer pipette and inserted into the 24% Percoll such that the tip touched the bottom of the tube at a slight angle. The 40% Percoll was then introduced slowly to the bottom to create two distinct layers in the solution.

After centrifugation the pellet was dislodged, resuspended in 3.5 ml of 15% Percoll using a plastic transfer pipette and slowly layered above the 24% Percoll. The introduction of the top layer was begun by leaning the tip of the pipette against the tube wall close to the surface of the 24% Percoll and adding slowly so that distinct layers would appear. To prepare one rat forebrain, two gradients in one tube each were prepared each time, so that one of the two could be used as centrifugation control.

Using the second tube as a balance tube, the Percoll gradients (one of them containing the homogenate) were centrifuged at 30,700 *g* at 4°C for 8 min using slow acceleration (45 s from 0 to 500 rpm followed by normal acceleration) and deceleration (no brakes), to redistribute the tissue material into three major bands (Figure 6). The material at the

top of the gradient – containing mostly myelin –, as well as the underlying layer – containing mostly synaptosomes – was removed with an adjustable 1 ml volumetric pipette. Using the 1 ml volumetric pipette, the Percoll solution containing material accumulating at the interface between the 24% and 40% Percoll solution – which is enriched by non-synaptic mitochondria – was collected and added into a separate centrifuge tube. After adding ~6 ml of IB into this tube it was centrifuged at 16,700 *g* at 4°C for 10 min. The mitochondria would then be at the bottom of the tube as a loose pellet. The supernatant was poured off carefully, the resulted pellet was resuspended in ~1 ml of IB, and another ~10 ml of buffer were added. The mitochondria fraction was centrifuged again at 6,900 *g* at 4°C for 10 min. The supernatant was decanted and any remaining solution was removed from the wall of the centrifuge tube. The pellet was gently resuspended in 0.25 ml of IB, put into a 1.5 ml tube and kept on ice.

2.6 Determination of Mitochondrial Protein Concentration

After having isolated the mitochondria the protein concentration had to be determined in order to afterwards dilute the sample to a desired experimental concentration. This was done using the Bio-Rad Protein Assay – Standard Procedure for Microtiter Plates based on the dye-binding method of [66]: Using pure IB as blank and bovine serum albumin (BSA) samples in concentrations ranging from 1 mg to 10 mg per ml IB as

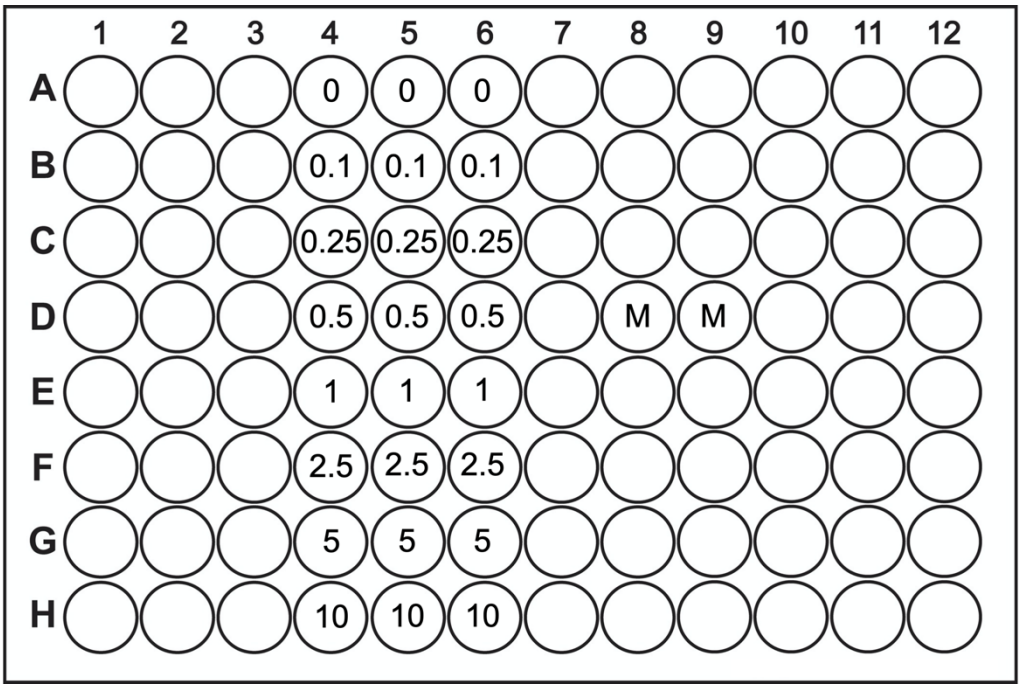

Figure 7: Plating Template for Bio-Rad Protein Assay
The mitochondrial protein concentration was determined by plotting mitochondrial samples (M) against bovine serum albumin sample standards of the shown concentrations (in mg ml^{-1}).

standards, 2 µl of each sample (including the mitochondria sample) were pipetted into a well of a 96-well-plate following Figure 7. 200 µl of diluted Bio-Rad Protein Assay Dye Reagent Concentrate (1:5 dilution in distilled, deionized water, filtered through a Corning® bottle-top vacuum filter) were then added to each well. The plate was incubated for at least 5 but not more than 60 min and shaken on a Microplate Shaker at 300 rpm. Finally, the absorbance was measured in a spectrophotometer at 595 nm. The mitochondria sample concentration was determined by plotting the standard absorbances (after subtracting the blank absorbance) to the standard concentrations and calculating a regression line by which the mitochondrial sample absorbance could be transferred into a concentration.

2.7 Injury of Mitochondria

2.7.1 In Vitro with Hydrogen Peroxide

One approach to injure mitochondria was to apply H_2O_2 on isolated mitochondria for a certain period of time. Preliminary data produced in the Riess Lab suggested that a concentration of 200 µM for 10 min would be sufficient to decrease mitochondrial viability by 50% [67]. After having determined the mitochondrial protein concentration, the mitochondria sample was taken out of the ice-cold surrounding into RT and H_2O_2 was added to result in 200 µM H_2O_2 in mitochondrial solution. The mitochondria sample was then incubated for 10 min on a Microplate Shaker at 500 rpm. A control mitochondria sample was incubated the same way without H_2O_2.

2.7.2 In Vivo by Asphyxial Cardiac Arrest

The other approach to injure mitochondria was to induce an in vivo asphyxial cardiac arrest in rats in contrast to the H_2O_2-induced injury in vitro. For this purpose – after induction of general anesthesia (cf. 2.4.2 Animal Preparation for Asphyxial Cardiac Arrest) – cardiac arrest was achieved following a protocol modified from Katz et al. [68]. After preparation and a stabilization phase of 30 min, 3 mg kg^{-1} of the neuromuscular blocker rocuronium bromide (Hospira, Inc., Lake Forest, IL, USA) was given intravenously. Then, 2 min later, the ventilation was stopped, thus inducing asphyxia. This reliably resulted in a cardiac arrest after ~3 min, which was defined as a systolic blood pressure less than 20 mmHg. Asphyxial cardiac arrest was maintained for 15 min. Sham control rats underwent the same procedure, but without sustaining asphyxia and cardiac arrest. Immediately after the defined time of asphyxia, the

anesthetized animal was euthanized by decapitation and the mitochondria isolated (cf. 2.4.3 Euthanization and Brain Extraction and 2.5 Isolation of Mitochondria).

2.8 Treatment with Poloxamer 188

2.8.1 Treatment after Hydrogen Peroxide-Induced In Vitro Injury

The treatment with P188 after H_2O_2-induced injury (cf. 2.7.1 In Vitro with Hydrogen Peroxide) occurred in two different options: P188 was applied in a final concentration of 250 µM by diluting the mitochondria sample 1:2 with 500 µM P188 in EB and hereby also slowing down the reaction of H_2O_2. After diluting, the sample was either placed back on ice or shaken at 500 rpm at RT for 10 more min until it was placed on ice as well. Combined with the 10 min of RT during the H_2O_2-induced injury this resulted in two different times of exposure to RT (10 min RT; 20 min RT). A control mitochondria sample would undergo a 1:2 dilution with plain EB and would as well be placed on ice immediately or after 10 min (Figure 8).

2.8.2 Treatment after Asphyxial Cardiac Arrest-Induced In Vivo Injury

Brain mitochondria of a rat which had undergone asphyxial cardiac arrest (cf. 2.7.2 In Vivo by Asphyxial Cardiac Arrest) were isolated, the protein concentration was determined, and the sample was diluted to 2 mg ml^{-1} protein concentration with ice-cold EB. 250 µM P188 was applied by diluting 1:2 with 500 µM P188 in EB. The sample was shaken at RT for 10 min and placed back on ice. A control mitochondria sample with plain EB was prepared the same way (Figure 9).

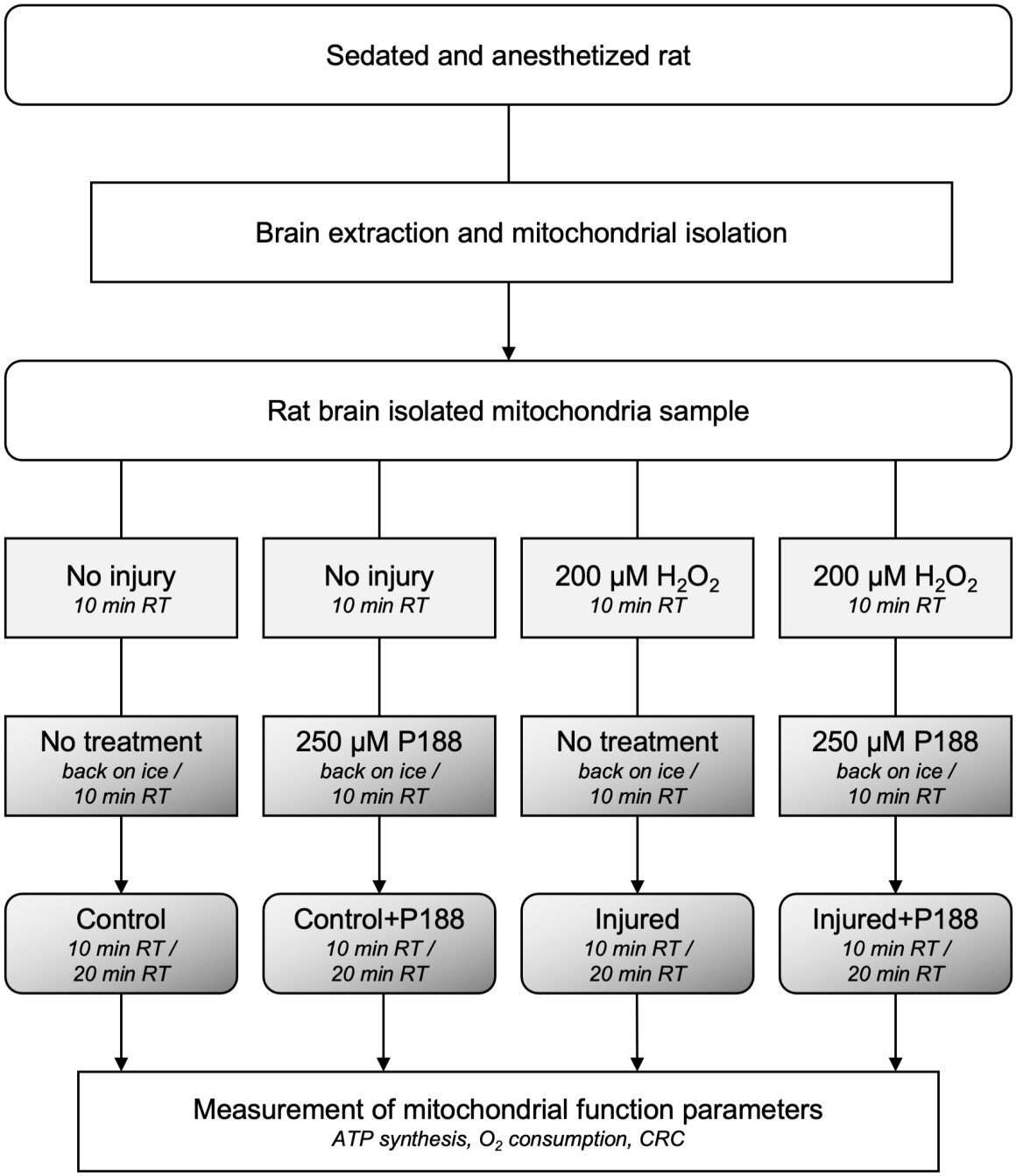

Figure 8: Experimental Set-up for Hydrogen Peroxide-Injured, Isolated Mitochondria

Rat brain mitochondria were isolated previously to being injured and continiously kept on ice. Injury with 200 µM hydrogen peroxide took place at room temperature (RT) for 10 min. For treatment with 250 µM Poloxamer (P)188 mitochondria were either put back on ice or kept at room temperature . This results in four different groups (control, control+P188, injured, injured+P188) which were exposed to a total of either 10 or 20 min RT (different grey shades depict total duration of RT, with darker shade corresponding to longer duration and mixed shades corresponding to two different durations in one group).

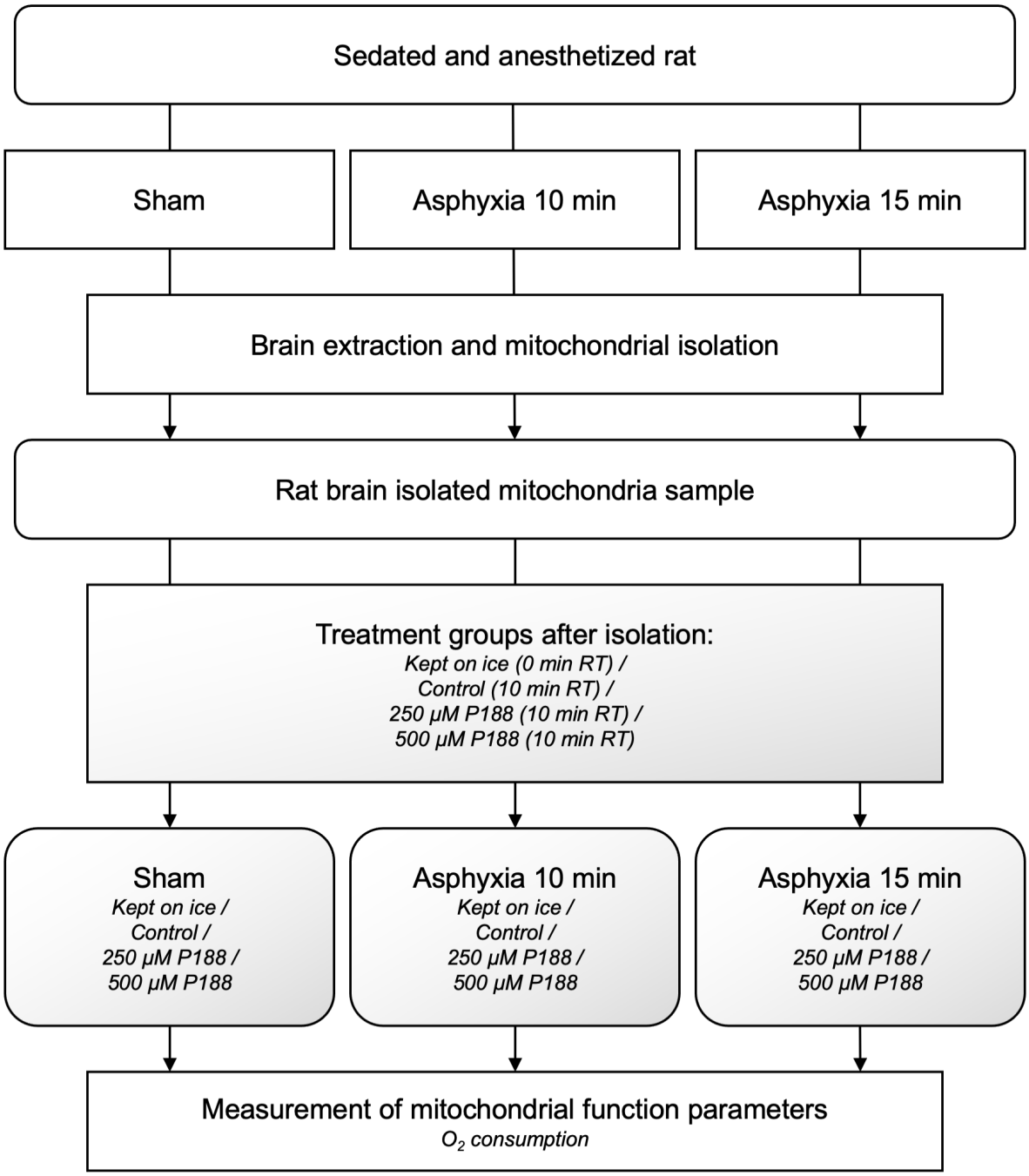

Figure 9: Experimental Set-Up for Cardiac Arrest-Injured, Isolated Mitochondria
Sedated and anesthetized rats were submitted to sham conditions, or asphyxia of 10 or 15 min – which resulted in cardiac arrest – previously to brain extraction and mitochondrial isolation. For treatment with 250 or 500 µM Poloxamer (P)188 mitochondria were kept at room temperature (RT) for 10 min. Control mitochondria were exposed to RT but not to P188 and the fourth condition consisted of mitochondria continuously kept on ice. This results in three different groups (sham, asphyxia 10 min, asphyxia 15 min) with four conditions each (different grey shades depict total duration of RT, with darker shade corresponding to longer duration and mixed shades corresponding to two different durations in one group).

2.9 Measurement of Mitochondrial Function Parameters

Three methods were used to assess mitochondrial viability: ATP synthesis, O_2 consumption and CRC. They have been described before [45,69–71].

2.9.1 Adenosine Triphosphate Synthesis Assay

The ATP Assay buffer – containing ADP, DAP, luciferin, and luciferase (Firefly-Enzyme) (for exact concentrations cf. 2.2 Buffers) – allows functional mitochondria to produce ATP, resulting in bioluminescence measured by a luminometer. Thus, the more ATP is produced, the more luminescence will be measured, indicating higher mitochondria viability (Figure 10).

A clear Eppendorf tube was filled with 500 µl of ATP assay buffer and placed in the luminometer. First 10 µl of mitochondria, then 5 µl of combined 0.5 M sodium glutamate/0.5 M disodium malate (complex I substrates) or 5 µl of 0.5 M succinate (complex II substrate) with 5 µl of 0.5 mM rotenone – depending on which complex was tested – were added, starting the reaction. The lid was closed and the measurement started by pressing the apposite button.

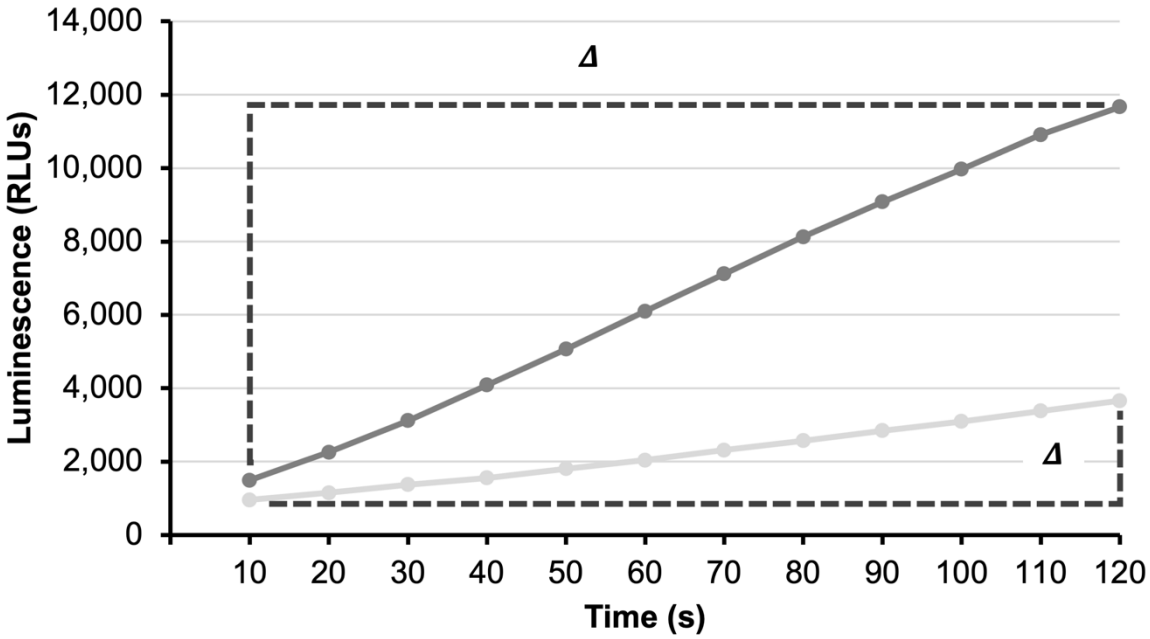

Figure 10: Differences in Adenosine Triphosphate Synthesis over Time
Mitochondrial adenosine triphosphate (ATP) synthesis is measured by the reaction of ATP with luciferase. With higher ATP synthesis, luciferase produces more light, which is measured by an increase in relative luminescence units (RLUs; compare dark grey to light grey lines). The difference (Δ) in RLUs over time determines the rate of ATP synthesis.

The rate of ATP produced was then calculated in µmol min^{-1} mg^{-1} by the rate of increase in luminescence in relation to a standard curve derived from known ATP concentrations ranging from 2.5 to 200 µM.

2.9.2 Oxygen Consumption Assay

To use this method a respiration chamber with a Clark-type electrode is required. The electrode is separated from the solution it is measuring by a fluorethylenpropylen (FEP) membrane and is able to quantify the O_2 concentration across it (Figure 11). The O_2 consumption by the mitochondria is therefore measurable and their viability determinable.

The Strathkelvin Mitocells containing the respiration chambers were connected to the Strathkelvin Dual Channel Meter and the Strathkelvin Oxygen Program started on the computer. The recording channel in the program was adjusted to the concentration of the mitochondria sample (cf. 2.6 Determination of Mitochondrial Protein Concentration) and to its volume (70 µl mitochondria). The cell stirrer was turned on.

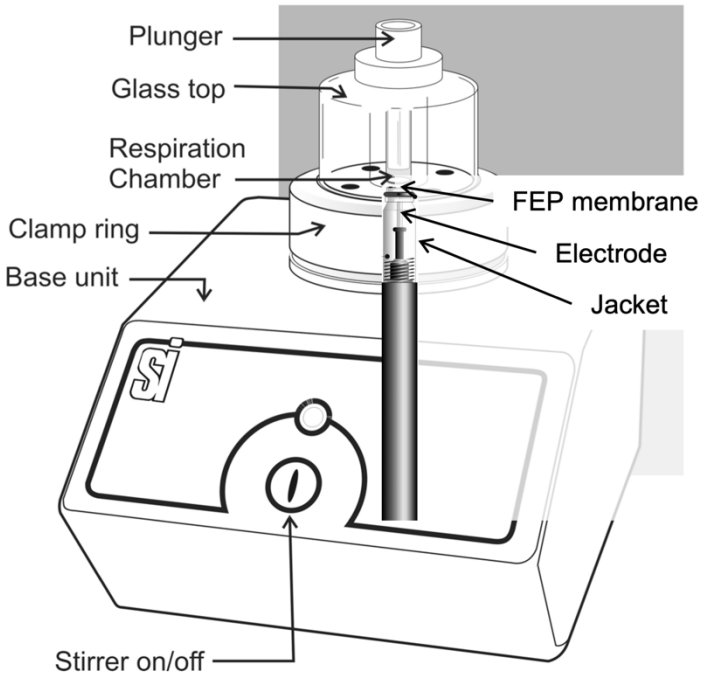

Figure 11: Strathkelvin Mitocell and Oxygen Electrode
The Mitocell consists of a base unit, which controls the magnetic stirrer and holds the oxygen electrode, and the glass top which forms the respiration chamber and holds a plunger on top. Base unit and glass top are connected through the clamp ring.
The electrode swims in a buffered potassium chloride solution and is covered by a jacket. The electrode is separated from the respiration chamber by the fluorethylenpropylen (FEP) membrane which is highly but selectively permeable for oxygen. According to Strathkelvin Instruments Limited [72,73]

$$RCI = \frac{\text{state 3}}{\text{state 4}}$$

Figure 12: Respiratory Control Index
The respiratory control index (RCI) is calculated by dividing the oxygen consumption in state 3 by the one in state 4.

280 µl EB and 70 µl mitochondria were introduced into the respiration chamber and the plunger was inserted into the chamber to close it. The O_2 concentration was measured for 60 s. Then either 3.5 µl of combined 1 M sodium glutamate and 1 M disodium malate solution (complex I substrates) or 3.5 µl of 1 M succinate (complex II substrate) with 3.5 µl of 1 mM rotenone – depending on which complex was tested – were added by introducing the apposite Hamilton syringes through the capillary in the plunger into the cell. This activated state 2 of mitochondrial respiration. After another 60 s, 3.5 µl of 25 mM ADP were added, again with the apposite Hamilton syringe. This started the state 3 respiration which is characterized by a higher O_2 consumption. The

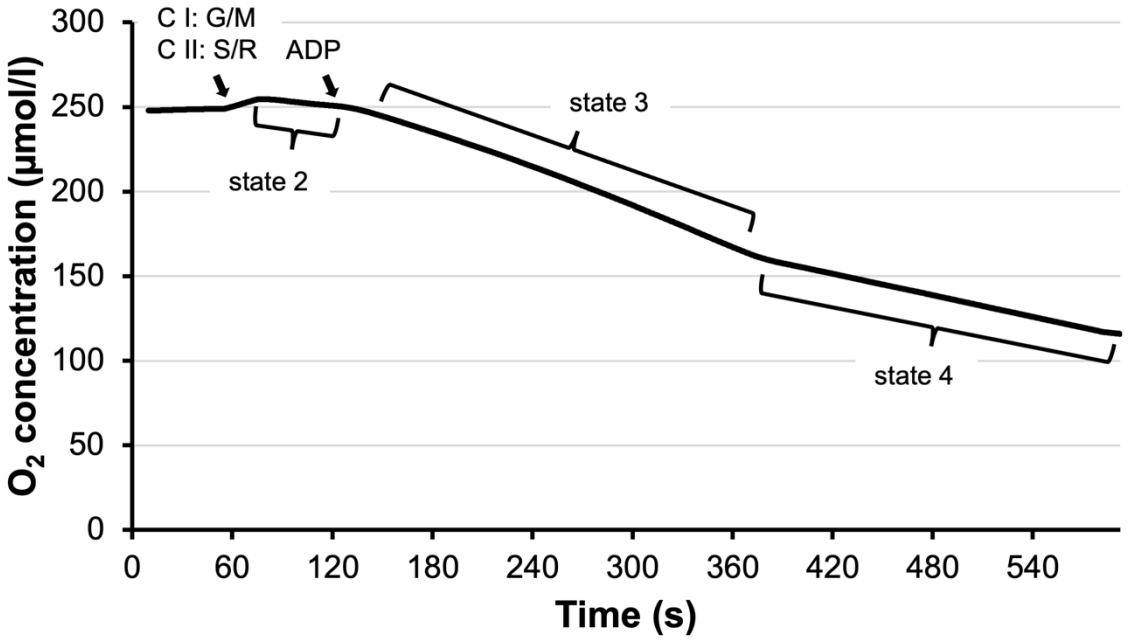

Figure 13: States of Mitochondrial Oxygen Consumption
Mitochondrial oxygen (O_2) consumption can be divided into different states. State 2 occurs, when substrates of the respiratory chain are present except for adenosine diphosphate (ADP). The substrates to fuel into complex I (C I) are glutamate/malate (G/M), while complex II (C II) is propelled by succinate (S) and isolated through blocking complex I with rotenone (R). State 3 is then started by adding ADP which enables the adenosine triphosphate synthase. When ADP is completely consumed, O_2 consumption switches into state 4.

O_2 concentration was observed until the O_2 consumption would decrease, signaling the beginning of state 4. From this point, the O_2 concentration was monitored for another minute before the recording was stopped.

Regression lines in the different states were calculated. By this, the O_2 consumption in state 3 and state 4 could be identified and the respiratory control index (RCI) determined (Figures 12 and 13).

2.9.3 Calcium Retention Capacity Assay

Similar to the endoplasmic reticulum, mitochondria are able to retain Ca^{2+} in order to maintain a low cytoplasmatic Ca^{2+} concentration [28]. The mitochondrial Ca^{2+} retention can lead to swelling of the mitochondria proportional to the Ca^{2+} retained. If too much Ca^{2+} is retained the mPTP will open and release the Ca^{2+}. The CRC assay works by using a Ca^{2+} binding fluorescent dye which cannot pass through the mitochondrial membrane. Ca^{2+} is added gradually to the solution and is retained by the mitochondria. When mPTP opens the released Ca^{2+} will bind the dye resulting in a fluorescent reaction which can be quantified.

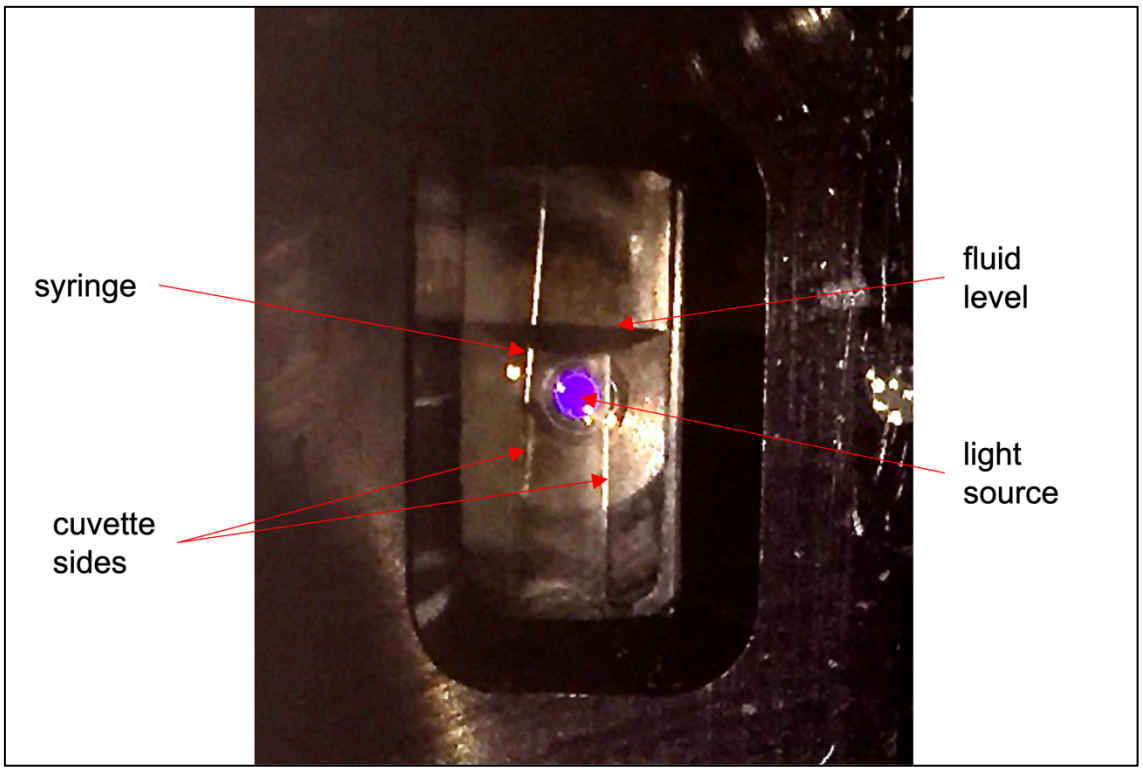

Figure 14: Needle Insertion during Calcium Retention Capacity Assay
The needle infusing the calcium chloride ($CaCl_2$) had to be inserted deep enough into the cuvette so that the $CaCl_2$ would not remain on top of the fluid level but instead be well mixed with the fluid in the cuvette. However, the needle was not allowed to cross the light path, therefore the needle was inserted at a slight angle to rest at the side of the cuvette.

The fluorescence spectrophotometer was switched on, igniting the bulb and letting it warm up for at least 10 min until a wattage of 70 W was reached. The voltage was checked not to surpass 14 V; if it did, the light bulb would have had to be changed. The slit widths were set on 299 nm and 210 nm. The Felix GX program was started and set on the Ca Green mode. A blank was run with plain EB. The excitation was set to 506 nm and the emission to 532 nm. The blank run usually should show a consistent emission of ~400 relative luminescence units (RLUs). Next 100 nM Calcium Green EB was measured, resulting in a consistent emission of ~10,000 RLUs. The apposite syringe, tubing and needle were filled with 1 mM $CaCl_2$ in no-phosphate EB ready to be infused into the cuvette later on.

450 µl of 100 nM Calcium Green EB and 50 µl mitochondria were added to the cuvette. The mixture of the different solutions was ensured by a stirrer on the bottom of the cuvette. Then either 5 µl of combined 1 M sodium glutamate and 1 M disodium malate solution (complex I substrates) or 5 µl of 1 M succinate (complex II substrate) with 5 µl of 1 mM rotenone – depending on which complexes were tested – were added. The

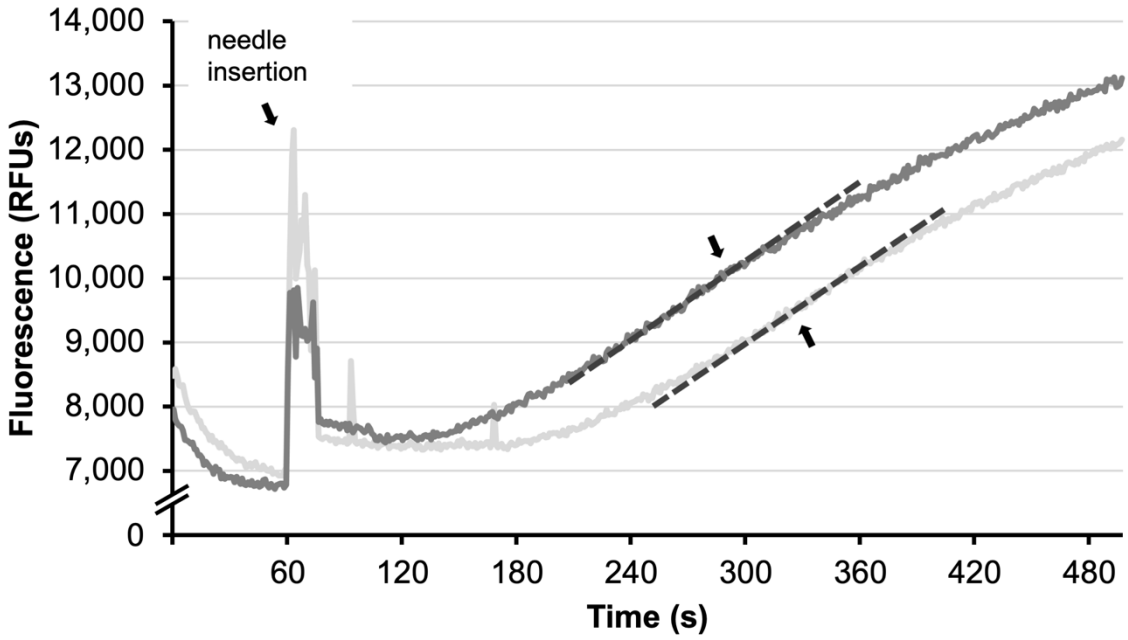

Figure 15: Mitochondrial Calcium Retention Capacity
Calcium retention capacity is defined as the maximal amount of calcium (Ca^{2+}) that can be kept inside mitochondria. With the insertion of the needle into the cuvette, calcium chloride is pumped at a continuous rate into the mitochondrial suspension. Extramitochondrial Ca^{2+} binds Calcium Green™. This results in increased fluorescence measured in relative fluorescence units (RFUs). The highest slope (dotted lines) indicated the moment at which mitochondrial permeability transition occurred in most mitochondria. This allowed calculation of the amount of Ca^{2+} infused into the mitochondrial suspension until this point.

lid was then closed and the recording started. After 60 s, the needle attached to the $CaCl_2$ filled syringe was inserted through the cone on top of the lid and the infusion pump started at 10 µl min^{-1}. It was of utmost importance to insert the needle in a way that the light path was not interrupted and that the infused $CaCl_2$ was well mixed with the fluids in the cuvette (Figure 14). After a short spike, the recording would show a steady state in which all the Ca^{2+} infused would be retained by the mitochondria (Figure 15). When MPT occurred, the Ca^{2+} released bound to the Calcium Green dye, and the resulting fluorescence would show increasing luminescence in the recording.

To determine CRC, the time point of the fastest increase, i.e., the steepest slope, was measured, when MPT was occurring in most mitochondria (Figure 15). This allowed the calculation of CRC as the amount of Ca^{2+} in µmol mg^{-1} infused into the mitochondrial suspension until this point.

2.10 Data Analysis and Statistics

Independently of the assay used to assess mitochondrial function, the resulting data were always controlled for normality with the Shapiro-Wilk test and for homoscedasticity (homogeneity of variance) with the Levene's test. If both tests were passed ($p>0.05$), data analyses were conducted through parametric testing. If one or both of them failed ($p<0.05$), non-parametric testing was performed.

For parametric testing, one-way ANOVA was performed to compare the means of the different groups. If a statistically significant difference ($p<0.05$) was detected, the Student-Newman-Keuls method was applied as a post-hoc test to detect between which groups the difference was.

If only the Levene's test but not the Shapiro-Wilk test failed, data were analyzed with tests which do not require homoscedasticity. These were namely the Welch's one-way ANOVA and the Games-Howell post-hoc test, the latter one only being used if significant differences ($p<0.05$) were detected.

For data that failed the Shapiro-Wilk test, the non-parametric Kruskal-Wallis test was performed. If significant differences ($p<0.05$) were found, the Wilcoxon rank-sum test was applied for post-hoc testing.

Graphically, statistically significant differences ($p<0.05$) are indicated by brackets or (*). Since not all data fulfilled the criteria for parametric testing, the results are presented as box plots to portray the data distribution accurately.

All data were analyzed using R [74] with the packages “car” [75], “dplyr” [76], “ggoubr” [77], “agricolae” [78], and “userfriendlyscience” [79].

3 Results

3.1 Isolated Mitochondria after In Vitro Hydrogen Peroxide-Induced Injury

Isolated mitochondria were incubated with 200 µM H_2O_2 for 10 min before being diluted with or without 250 µM P188. Thereafter, mitochondrial function parameters for complexes I and II substrates were assessed, specifically ATP synthesis, O_2 consumption and CRC. The results were stratified for the four groups that resulted from the injuring and treatment process (control, control+P188, injured, injured+P188). Throughout the course of the present study it became clear that the values produced would differ greatly between different experiment days, while being relatively comparable within the same experiment day. This was mainly attributed to improving technique of the researcher throughout the course of the present study. To account for these changes, percentages of the control on each experiment day were calculated, reducing the variance but not cancelling it completely. Therefore, not only absolute values but also percentages of control were discussed.

3.1.1 Adenosine Triphosphate Synthesis after Hydrogen Peroxide-Induced Injury

For complex I substrates, ATP synthesis of control mitochondria showed a median of 0.70 µmol min^{-1} mg^{-1} with an interquartile range from 0.55 to 1.61 µmol min^{-1} mg^{-1} (Figure 16A). When adding P188 to the control, ATP synthesis remained fairly equal to the control without P188, with no significant differences (Figure 16A). The ATP synthesis of injured mitochondria without P188 was significantly impaired compared to the control mitochondria with a median of 0.39 µmol min^{-1} mg^{-1} and an interquartile range from 0.31 to 0.49 µmol min^{-1} mg^{-1} (Figure 16A). This was, again, independent from P188 treatment as P188 did neither increase nor decrease ATP synthesis in injured mitochondria. However, although the ATP synthesis of mitochondria treated with P188 appeared to differ in control mitochondria compared to injured mitochondria with the medians being 0.77 µmol min^{-1} mg^{-1} and 0.48 µmol min^{-1} mg^{-1}, respectively, this is not statistically different (Figure 16A). The percentage values of ATP synthesis for complex I substrates present a similar image but with less variance: Control mitochondria showed 100% of ATP synthesis independently of incubation with or without P188 (Figure 17A). Injured mitochondria showed a statistically significant drop of ATP synthesis of approximately 40% to 70%, again, independently of the addition of P188 (Figure 17A).

For complex II substrate, ATP synthesis of control mitochondria showed a median of 0.12 µmol min^{-1} mg^{-1} with an interquartile range from 0.11 to 0.60 µmol min^{-1} mg^{-1} (Figure 16B). The addition of P188 did not significantly affect ATP synthesis of control mitochondria with median ATP synthesis being at 0.10 µmol min^{-1} mg^{-1} (Figure 16B). Median ATP synthesis of injured mitochondria was not markedly different compared to control mitochondria, however, the interquartile range was strongly reduced ranging from 0.08 to 0.14 µmol min^{-1} mg^{-1} (Figure 16B). The same applies for injured mitochondria with added P188, where the interquartile range of ATP synthesis ranged from 0.06 to 0.17 µmol min^{-1} mg^{-1} (Figure 16B). However, the difference in ATP synthesis of injured mitochondria compared to control mitochondria was not significant and this was independent of the addition of P188 (Figure 16B). The percentage values of ATP synthesis for complex II substrate, however, revealed significant differences in ATP synthesis between the different groups: Control mitochondria showed an ATP synthesis of 100%, but when P188 was added ATP synthesis significantly decreased to approximately 80% (Figure 17B). ATP synthesis in injured mitochondria was further decreased significantly to approximately 60% compared to control mitochondria without P188 (Figure 17B). When P188 was added to injured mitochondria, it caused a reduction of ATP synthesis to 50% compared to control mitochondria (Figure 17B). ATP synthesis in P188-treated injured mitochondria was significantly impaired compared to control mitochondria not only without but also with P188 treatment (Figure 17B).

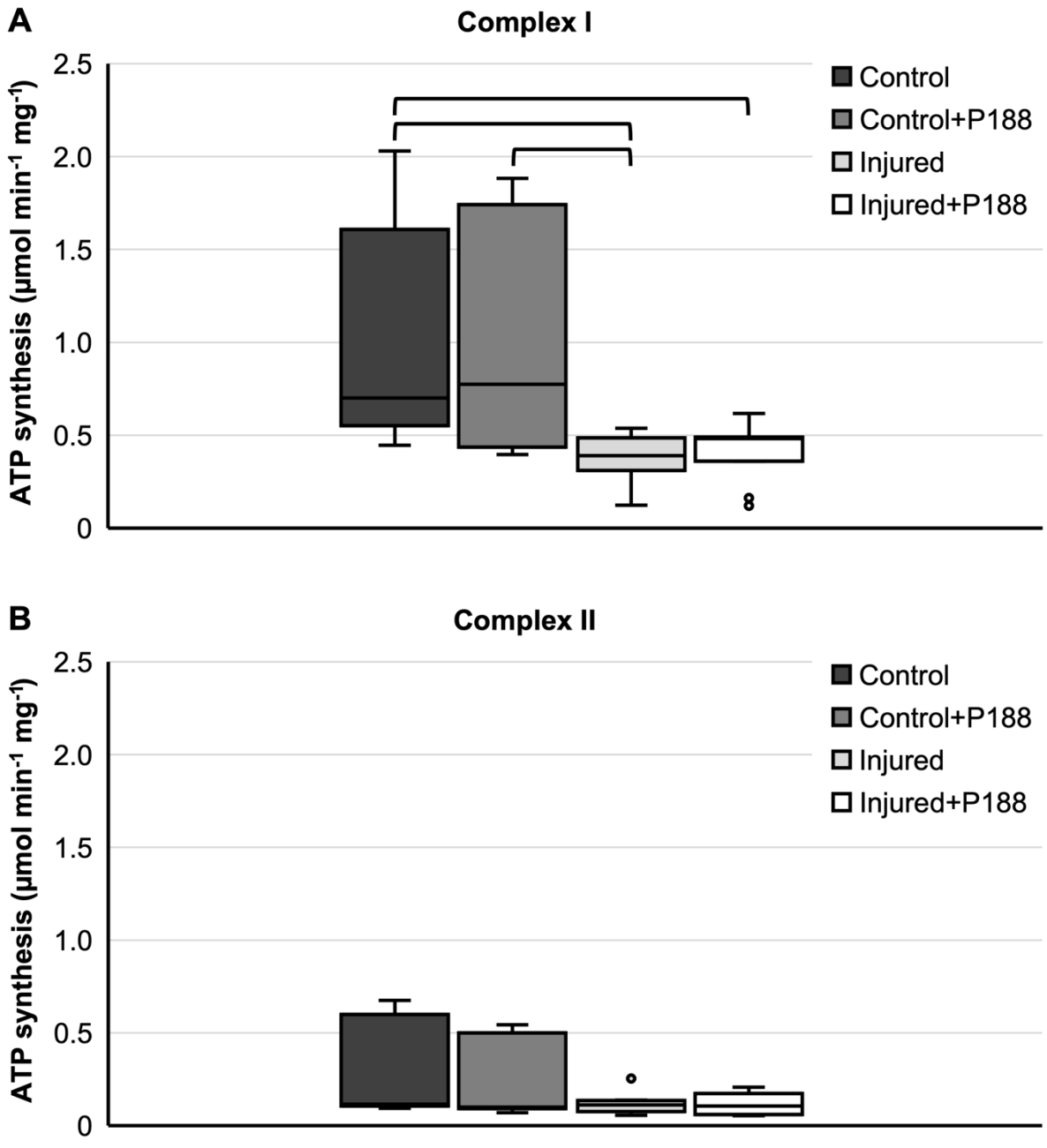

Figure 16: Adenosine Triphosphate Synthesis (µmol min^{-1} mg^{-1}) in Hydrogen Peroxide-Injured, Isolated Mitochondria

Adenosine triphosphate (ATP) synthesis for complex I (A) and II (B) substrates is compared for control, control+Poloxamer (P)188, injured, and injured+P188 mitochondria groups. Whiskers represent minimum and maximum. Statistical significance ($p<0.05$) denotated through brackets; complex I: n=5, complex II: n=5.

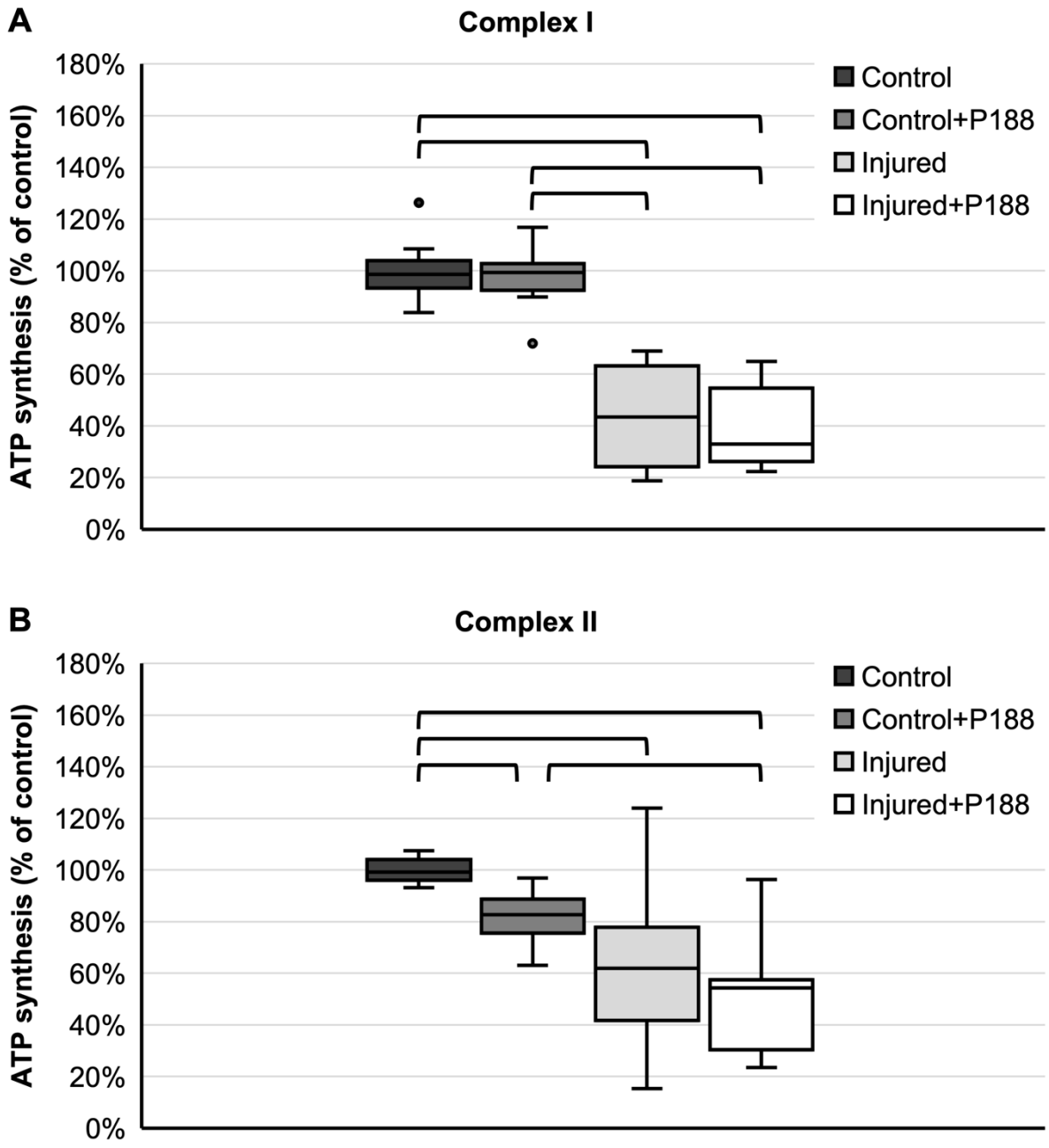

Figure 17: Adenosine Triphosphate Synthesis (% of Control) in Hydrogen Peroxide-Injured, Isolated Mitochondria

Adenosine triphosphate (ATP) synthesis for complex I (A) and II (B) substrates is compared for control, control+Poloxamer (P)188, injured, and injured+P188 mitochondria groups. Whiskers represent minimum and maximum. Statistical significance ($p<0.05$) denotated through brackets; complex I: n=5, complex II: n=5.

3.1.2 Oxygen Consumption after Hydrogen Peroxide-Induced Injury

Median O_2 consumption of control mitochondria for complex I substrates was at an RCI of 1.37, the interquartile range ranged from 1.28 to 1.43 (Figure 18A). The addition of P188 to control mitochondria caused a slightly higher RCI at a median of 1.40 and an interquartile range from 1.37 to 1.51 (Figure 18A). Median O_2 consumption at 1.34 of injured mitochondria without P188 treatment was fairly equal to control mitochondria. The interquartile range of injured mitochondria from 1.13 to 1.40 extended markedly lower than the interquartile range of control mitochondria (Figure 18A). With a median of 1.19 and an interquartile range from 1.17 to 1.21 O_2 consumption of injured mitochondria treated with P188 was strongly decreased compared to the other mitochondrial groups (Figure 18A). However, these differences were not statistically significant (Figure 18A). The percentage values of O_2 consumption for complex I substrates present a similar image: Median O_2 consumption of control mitochondria was at 100% and this was fairly equal in P188-treated control mitochondria and injured mitochondria without P188 treatment (Figure 19A). However, injured mitochondria treated with P188 showed a reduction of 10% down to 90% of O_2 consumption, and, in contrast to the absolute values, this reduction was significantly different to P188-treated control mitochondria (Figure 19A).

For complex II substrate, control mitochondria showed a median O_2 consumption at an RCI of 1.39 with an interquartile range from 1.34 to 1.46 (Figure 18B). The addition of P188 to control mitochondria did not significantly change O_2 consumption (Figure 18B). O_2 consumption of injured mitochondria without P188 treatment was reduced to 1.29, and this was significantly different compared to control mitochondria without P188 treatment (Figure 18B). The addition of P188 to injured mitochondria again led to a decrease of O_2 consumption to 1.18 and this was significantly different compared to control mitochondria not only without but also with P188 treatment (Figure 18B). The percentage values of O_2 consumption for complex II substrate present a different picture: Control mitochondria with P188 treatment showed a significant reduction of O_2 consumption to approximately 95% compared to the 100% in control mitochondria without P188 treatment (Figure 19B). Injured mitochondria showed a significant decrease of O_2 consumption to 90% and 85% without and with P188 treatment, respectively, and this was significantly different compared to control mitochondria without P188 treatment (Figure 19B).

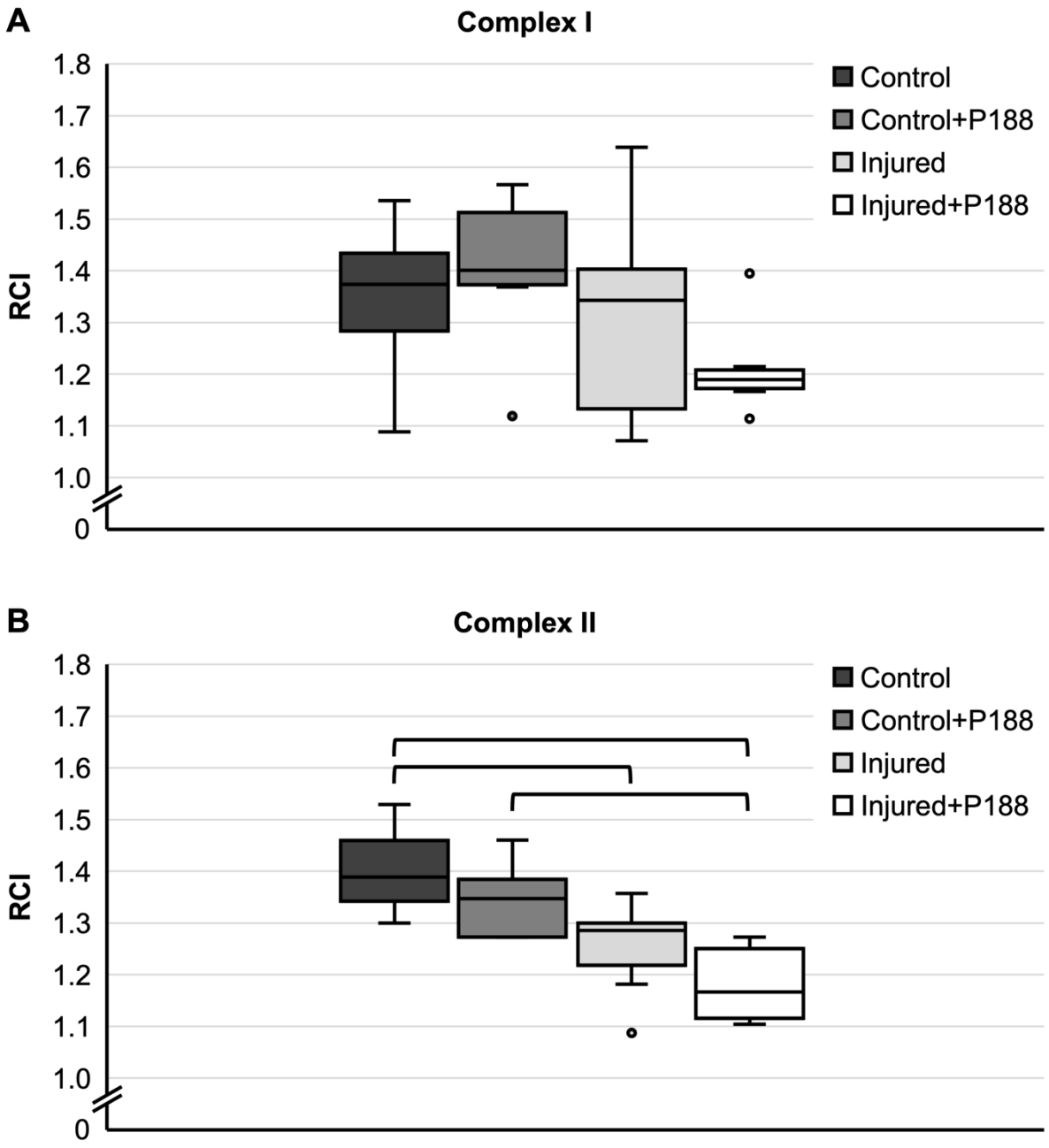

Figure 18: Respiratory Control Index of Oxygen Consumption in Hydrogen Peroxide-Injured, Isolated Mitochondria

Respiratory control index (RCI) of oxygen consumption for complex I (A) and II (B) substrates is compared for control, control+Poloxamer (P)188, injured, and injured+P188 mitochondria groups. Whiskers represent minimum and maximum. Statistical significance ($p<0.05$) denotated through brackets; complex I: n=6, complex II: n=5.

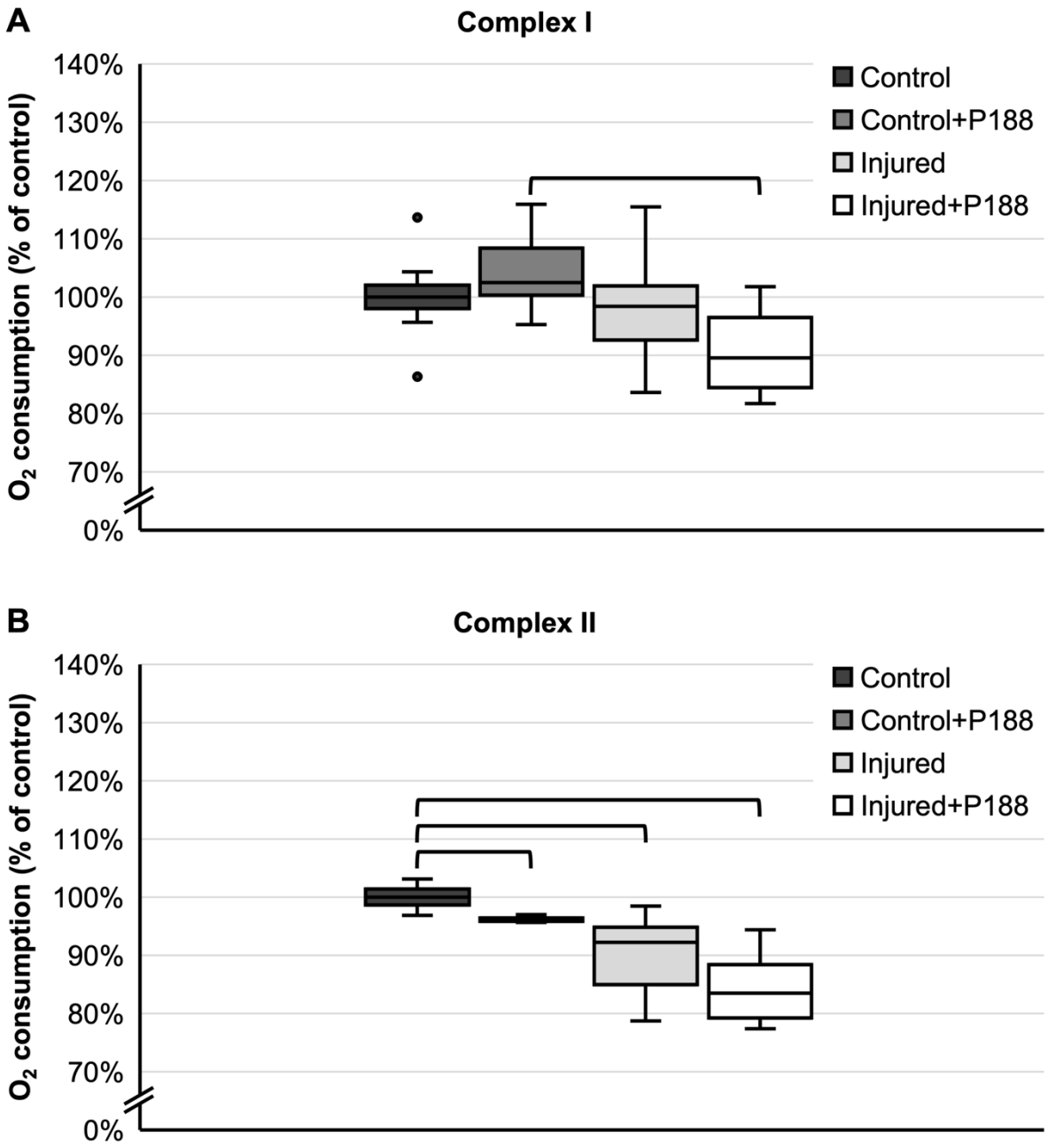

Figure 19: Oxygen Consumption (% of Control) in Hydrogen Peroxide-Injured, Isolated Mitochondria

Oxygen (O_2) consumption for complex I (A) and II (B) substrates is compared for control, control+Poloxamer (P)188, injured, and injured+P188 mitochondria groups. Whiskers represent minimum and maximum. Statistical significance ($p<0.05$) denotated through brackets; complex I: n=6, complex II: n=5.

3.1.3 Calcium Retention Capacity after Hydrogen Peroxide-Induced Injury

For complex I substrates, control mitochondria showed a median CRC of 0.35 µmol mg^{-1} and an interquartile range from 0.32 to 0.40 µmol mg^{-1} (Figure 20A). The addition of P188 to control mitochondria as well as the injury with H_2O_2 did not significantly change CRC (Figure 20A). The percentage values yielded similar results: P188-treated control mitochondria as well as untreated injured mitochondria showed a CRC of approximately 90% compared to control mitochondria without P188 treatment (Figure 21A). Injured mitochondria with P188 also showed a median CRC of around 90% (Figure 21A). However, the interquartile range of P188-treated injured mitochondria from approximately 70% to 100% extended lower compared to control mitochondria without P188 at an interquartile range from around 90% to 110% (Figure 21A). Although no significant differences were detected, in this case a trend is noticeable (Figure 21A).

For complex II substrate, control mitochondria showed a median CRC of 0.42 µmol mg^{-1} and an interquartile range from 0.33 to 0.47 µmol mg^{-1} (Figure 20B). With a median of 0.40 µmol mg^{-1} CRC of P188-treated control mitochondria was slightly but not significantly lower than control mitochondria without P188 (Figure 20B). Injured mitochondria showed a median CRC of 0.30 µmol mg^{-1} and 0.27 µmol mg^{-1} without and with P188, respectively, and this was significantly lower than control mitochondria independently of treatment with P188 (Figure 20B). However, this does not apply to the percentage values where no significant differences were found between the different groups: Median CRC of control mitochondria with P188 was at 93% and the interquartile range from 70% to 105% compared to control mitochondria without P188 with the median at 100% and the interquartile range from 99% to 101% (Figure 21B). At 71% and 61% without and with P188, respectively, median CRC of injured mitochondria was lower compared to control mitochondria (Figure 21B). However, the interquartile range of CRC in injured mitochondria still reached to over 100% (Figure 21B).

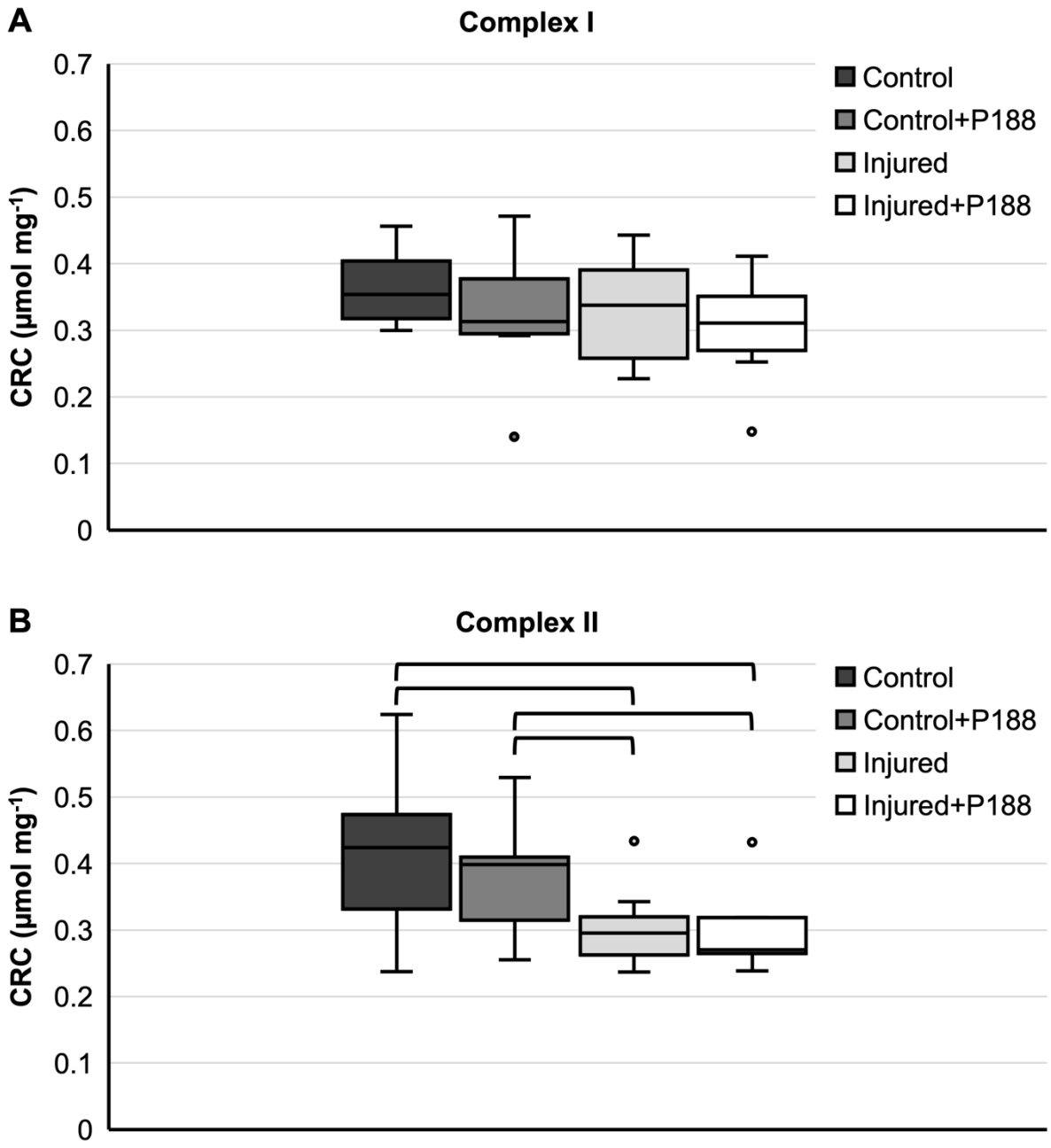

Figure 20: Calcium Retention Capacity (µmol mg^{-1}) in Hydrogen Peroxide-Injured, Isolated Mitochondria

Calcium retention capacity (CRC) for complex I (A) and II (B) substrates is compared for control, control+Poloxamer (P)188, injured, and injured+P188 mitochondria groups. Whiskers represent minimum and maximum. Statistical significance ($p<0.05$) denotated through brackets; complex I: n=4, complex II: n=5.

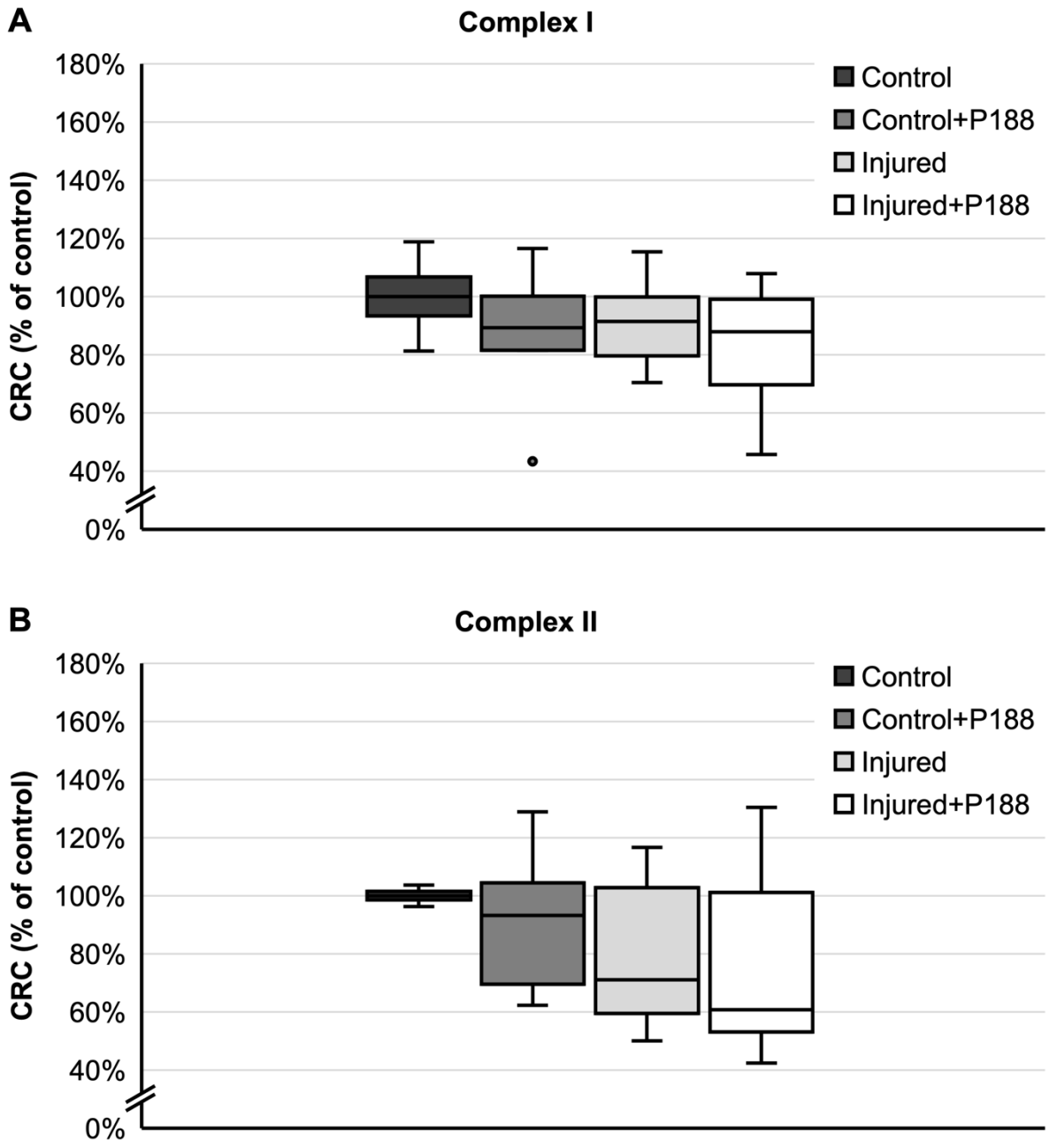

Figure 21: Calcium Retention Capacity (% of Control) in Hydrogen Peroxide-Injured, Isolated Mitochondria

Calcium retention capacity (CRC) for complex I (A) and II (B) substrates is compared for control, control+Poloxamer (P)188, injured, and injured+P188 mitochondria groups. Whiskers represent minimum and maximum. Complex I: n=4, complex II: n=5.

3.2 Comparison of Different Times of Exposure to Room Temperature on Isolated Mitochondria

Throughout the course of the experiments two different treatment regimens were executed in H_2O_2-injured, isolated mitochondria (cf. 2.8.1 Treatment after Hydrogen Peroxide-Induced In Vitro Injury). The main setting has already been thoroughly presented above (cf. 3.1 Mitochondrial Function Parameters after Hydrogen Peroxide-Induced Injury) and consisted of 10 min of exposure to H_2O_2 at RT and further 10 min RT after dilution with or without P188, summing up to a total of 20 min of exposure to RT (20 min RT). In the second setting the isolated mitochondria were immediately placed on ice after the 10 min of H_2O_2-induced injury at RT (10 min RT). Although the 20 min RT setting represents a more realistic simulation of I/R injury the 10 min RT shortens the exposure of isolated mitochondria to RT. Therefore, the two settings were compared to present the effects of prolonged exposure to RT on the isolated mitochondria.

The results within the 20 min RT condition have been presented above (cf. 3.1.3 Adenosine Triphosphate Synthesis after Hydrogen Peroxide-Induced Injury and 3.1.4 Oxygen Consumption after Hydrogen Peroxide-Induced Injury).

After 10 min RT median ATP synthesis of control mitochondria for complex I substrates was at 3.0 µmol min^{-1} mg^{-1} and 3.2 µmol min^{-1} mg^{-1} without and with P188, respectively (Figure 22A). Injured mitochondria showed a significantly lower ATP synthesis than control mitochondria at a median of 1.1 µmol min^{-1} mg^{-1} without as well as with P188 (Figure 22A).

For complex II substrate, median ATP synthesis after 10 min RT was at 0.6 µmol min^{-1} mg^{-1} in control mitochondria independently of the treatment with P188 (Figure 22B). Median ATP synthesis of injured mitochondria without P188 was at 0.5 µmol min^{-1} mg^{-1} and with that slightly but significantly lower than control mitochondria without P188 (Figure 22B). At a median of 0.4 µmol min^{-1} mg^{-1}, ATP synthesis of P188-treated injured mitochondria was significantly lower than control mitochondria, independently of the treatment with P188 (Figure 22B).

ATP synthesis for both complex I and II substrates was significantly decreased under 20 min RT compared to 10 min RT incubation in all four treatment groups, respectively (Figure 22).

After 10 min RT, median O_2 consumption of control mitochondria for complex I substrates was at an RCI of 2.6 independently of the treatment with P188. Compared

to control mitochondria, median O_2 consumption of injured mitochondria was decreased to an RCI of 1.9 and 2.0 without and with P188, respectively (Figure 23A). For complex II substrate, median O_2 consumption after 10 min RT was at an RCI of 1.4 and 1.3 in control mitochondria without and with P188, respectively (Figure 23B). Compared to control mitochondria, median O_2 consumption of injured mitochondria was slightly decreased to an RCI of 1.2 independently of treatment with P188 (Figure 23B).

O_2 consumption after 10 min RT was not statistically analyzed due to partially insufficient sampling (n=2), therefore no significant differences could be found. However, the data shows that O_2 consumption appeared to be, similarly to ATP synthesis, strongly affected by RT. This was mainly observable for complex I substrates where the RCI appeared diminished from 2.6 in the control mitochondria of the 20 min RT condition to 1.4 in the control of 10 min RT (Figure 23A).

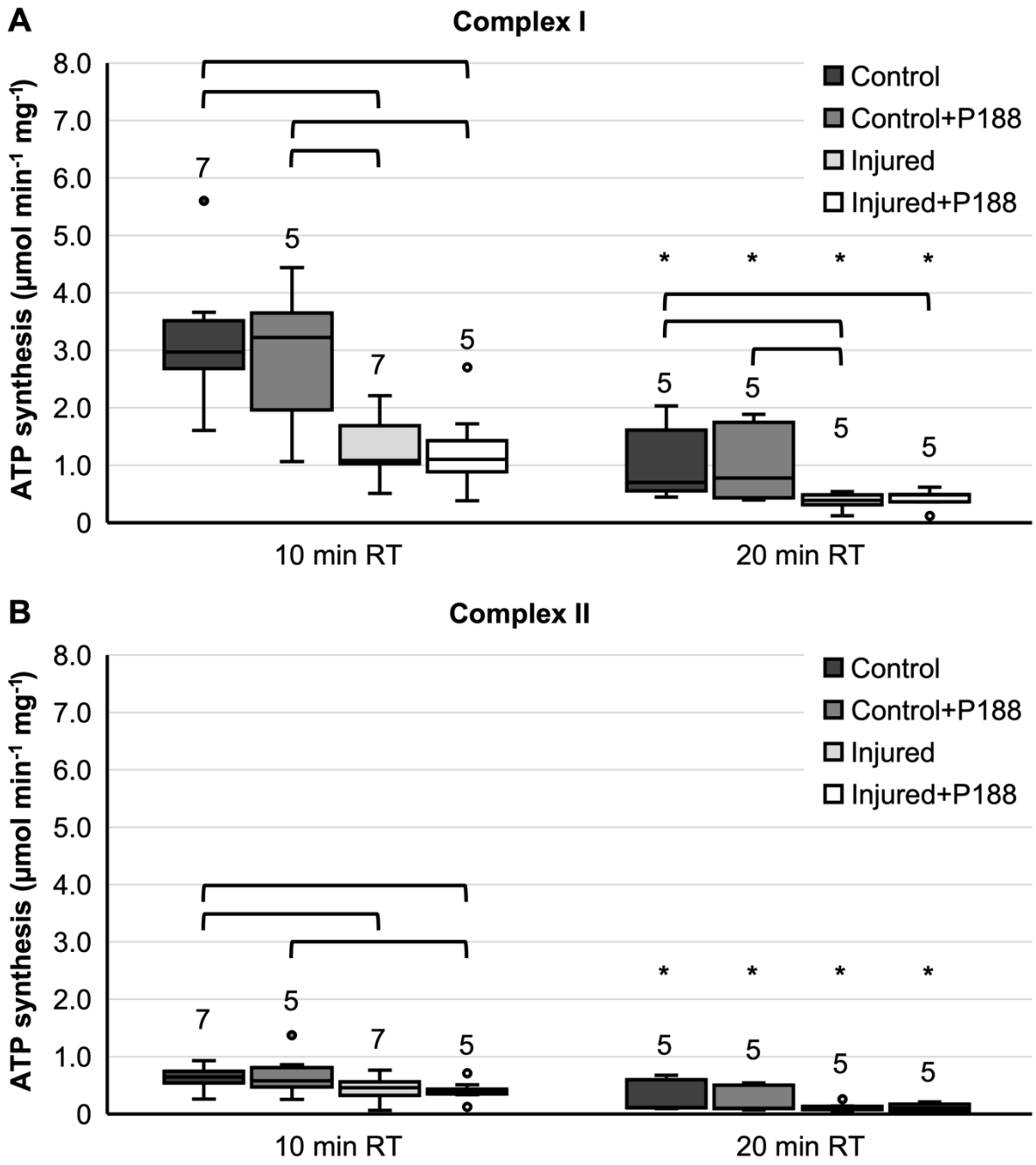

Figure 22: Comparison of Adenosine Triphosphate Synthesis (µmol min^{-1} mg^{-1}) between Differently Treated Hydrogen Peroxide-Injured, Isolated Mitochondria
Adenosine triphosphate (ATP) synthesis for complex I (A) and II (B) substrates is compared for control, control+Poloxamer (P)188, injured, and injured+P188 mitochondria groups. Condition is defined by total time of exposure of isolated mitochondria to room temperature (RT). Whiskers represent minimum and maximum. Statistical significance ($p<0.05$) within one condition was denotated through brackets; statistical significance ($p<0.05$) between the same groups of different conditions was denotated through (*); n depicted over its corresponding boxplot.

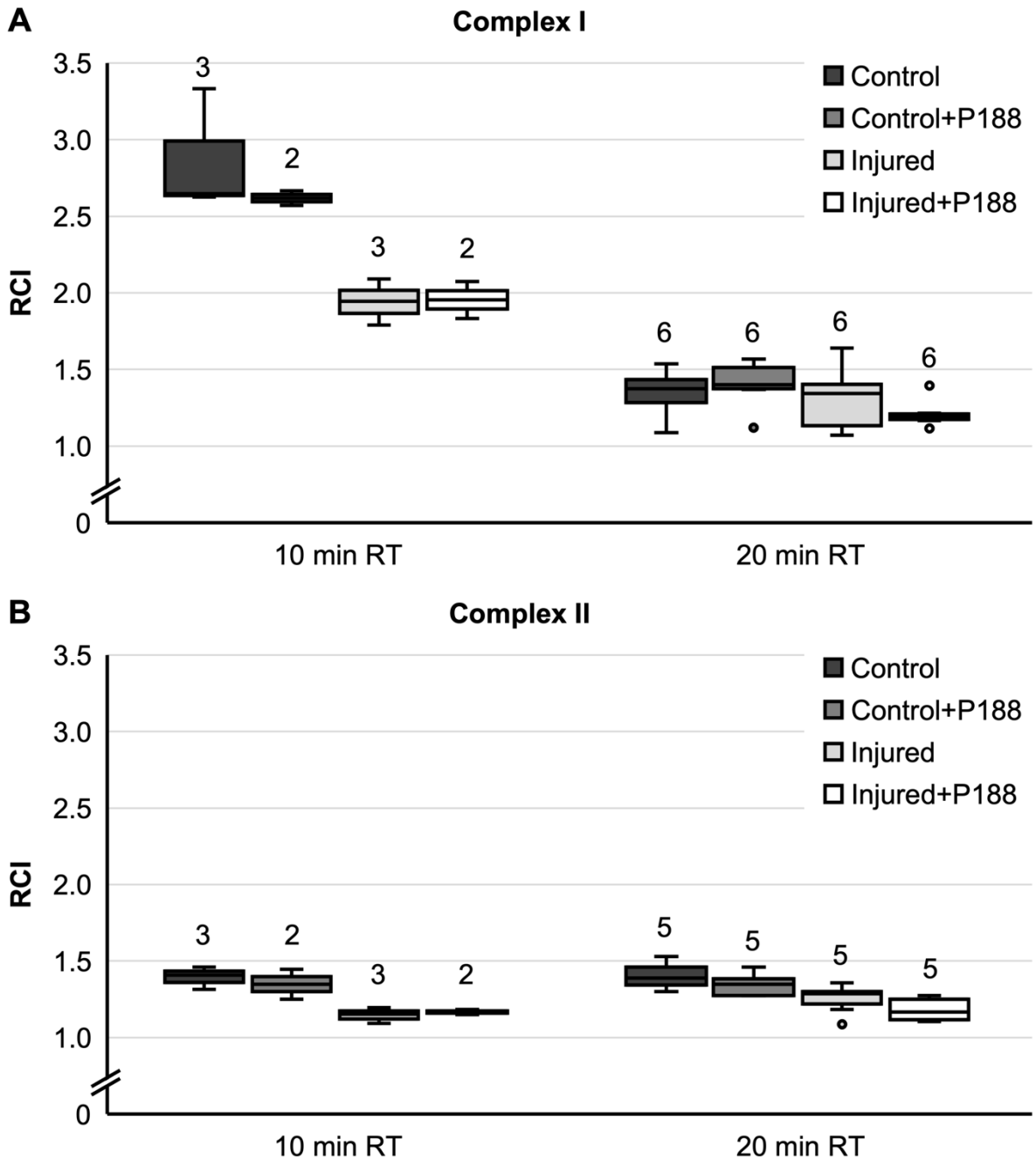

Figure 23: Comparison of Respiratory Control Indices of Oxygen Consumption between Differently Treated, H_2O_2-Injured, Isolated Mitochondria

Respiratory control index of oxygen consumption for complex I (A) and II (B) substrates is compared for control, control+P188, injured, and injured+P188 mitochondria groups. Condition is defined by total time of exposure of isolated mitochondria to room temperature (RT). Whiskers represent minimum and maximum; n depicted over its corresponding boxplot.

3.3 Isolated Mitochondria after In Vivo Asphyxial Cardiac Arrest-Induced Injury

In addition to the in vitro application of H_2O_2 an in vivo injuring strategy was applied in the experiments of the present study. This was done to account for the missing intracellular but extramitochondrial processes during ischemia. For this purpose, asphyxial cardiac arrest was induced in rats for either 10 or 15 min. Sham rats were only intubated and ventilated for 15 min. The animals were then euthanized and the forebrain mitochondria isolated. Subsequently, the mitochondria were either diluted with 250 µM P188, 500 µM P188 or just EB (control), and kept at RT for 10 min, or kept on ice completely, before assessing the O_2 consumption.

For complex I substrates, sham mitochondria (mitochondria from sham rats) that were completely kept on ice showed an RCI of 2.5 (Figure 24A). In mitochondria kept on ice, asphyxia of 10 and 15 min significantly decreased O_2 consumption to an RCI of 2.1 and 2.2, respectively (Figure 24A). Under sham conditions, control, 250 µM P188, and 500 µM P188 mitochondria showed significantly lower O_2 consumption at an RCI between 1.5 and 1.8 compared to sham mitochondria that was kept on ice (Figure 24A). Similarly, in the 15 min asphyxia condition O_2 consumption of control, 250 µM P188, and 500 µM P188 mitochondria was reduced to an RCI between 1.3 and 1.5 compared to mitochondria kept on ice (Figure 24A). While after 10 min asphyxia, O_2 consumption of control, 250 µM P188, and 500 µM P188 mitochondria appeared to be reduced to an RCI between 1.5 and 1.6 compared to the RCI of 2.1 in mitochondria kept on ice, no significant differences were detected (Figure 24A). Furthermore, with longer time of asphyxia a decrease of O_2 consumption in control, 250 µM P188, and 500 µM P188 mitochondria compared to the sham condition seemed observable, but this trend was, again, not significant (Figure 24A).

For complex II substrate, sham mitochondria that were completely kept on ice showed an RCI of 1.6 (Figure 24B). Asphyxia of 10 or 15 min led to an RCI of 1.5 and 1.8, respectively, with no significant differences found (Figure 24B). Control, 250 µM P188, and 500 µM P188 mitochondria showed no significant differences to each other or to mitochondria kept on ice neither within their condition nor outside (Figure 24B).

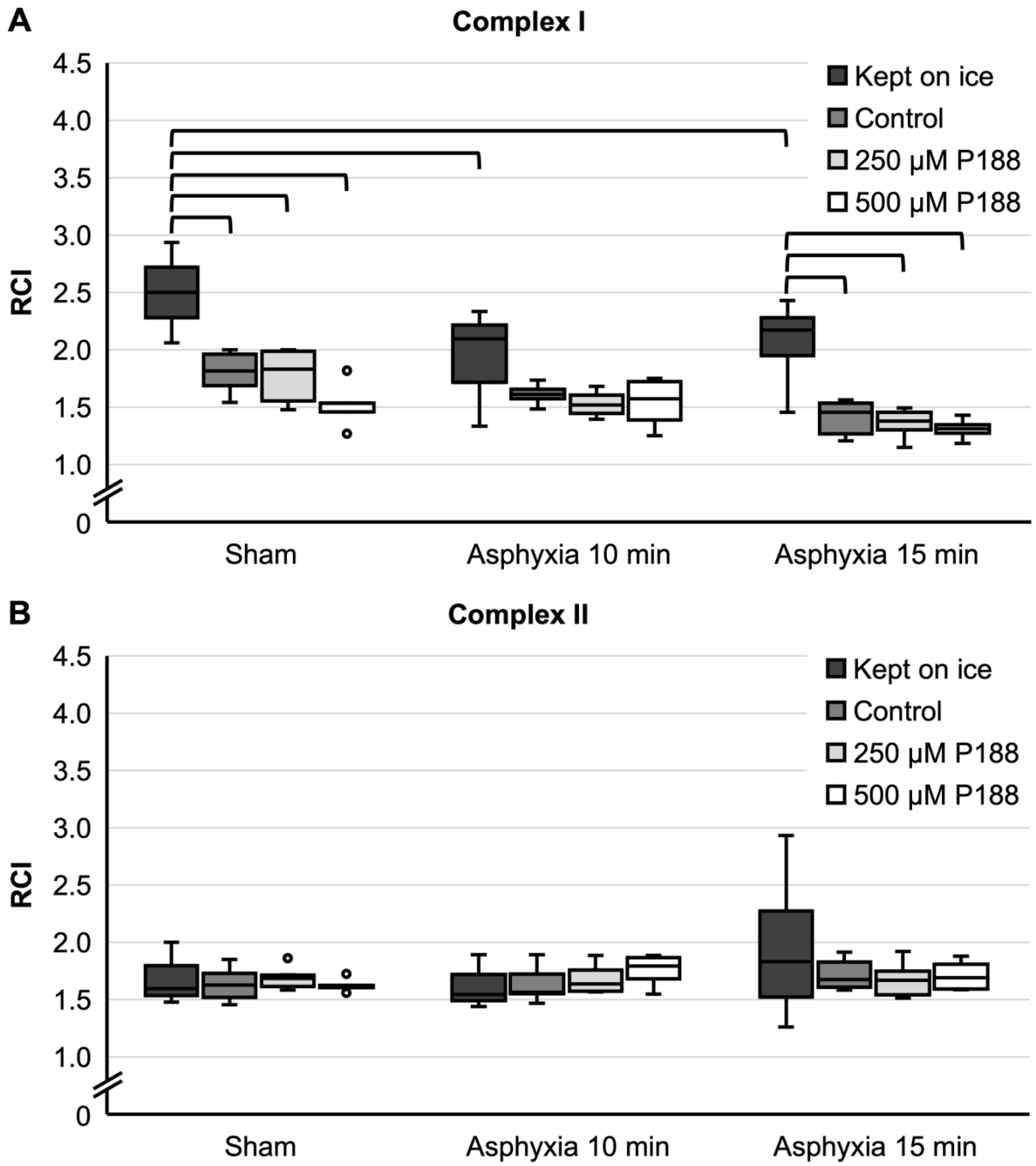

Figure 24: Respiratory Control Index of Oxygen Consumption of Cardiac Arrest-Injured, Isolated Mitochondria

Respiratory Control Index (RCI) of oxygen consumption for complex I (A) and II (B) substrates is compared for continuously kept on ice, control, treated with 250 µM P188, and treated with 500 µM P188 mitochondria groups. Prior to mitochondria isolation, asphyxial cardiac arrest had been induced in the rats with an asphyxial time of 10 or 15 min. A sham rat was ventilated throughout anesthesia without induction of asphyxia. Whiskers represent minimum and maximum. Statistical significance ($p<0.05$) denotated through brackets; complex I: n=3; complex II: n=3.

4 Discussion

4.1 Study Conclusions

The triblock copolymer P188 has been shown to rescue a variety of tissues and cell types from I/R injury in different settings (cf. 1.4 Poloxamer 188) [40–47,49,50,55,56,62]. Its structure, consisting of two hydrophilic chains with a hydrophobic center, enables P188 to stabilize damaged cell membranes by inserting its hydrophobic center into membrane pores [41]. More recently, profound improvements of mitochondrial function through P188 after I/R injury have become apparent [45,50,51,55,56,62,80], suggesting possibly a direct interaction of P188 with mitochondria, specifically by stabilizing their membrane.

In the present study a possible effect of P188 on rat isolated brain mitochondria after simulated I/R injury was examined. To recreate the I/R component of ROS directly in mitochondria, they were isolated from rat forebrains and exposed to 200 µM of H_2O_2 at RT for 10 min. In a second step, 250 µM P188 were added to the mitochondria which were then kept at RT for further 10 min to simulate reperfusion before finally assessing mitochondrial function through ATP synthesis, O_2 consumption, and CRC, each for complex I and II substrates, respectively. Data were not only analyzed in absolute values, but also in percentages of control to reduce variance between different experiment days.

In H_2O_2-injured, isolated mitochondria the absolute values show that ATP synthesis was significantly reduced for complex I substrates, while O_2 consumption and CRC were significantly reduced for complex II substrate. In addition, when analyzed as percentages of control, the data show significant injury through H_2O_2 for both complexes in ATP synthesis as well as O_2 consumption and no injury at all in CRC (cf. 3.1 Isolated Mitochondria after Hydrogen Peroxide-Induced Injury). Taken together, while not completely concordant for both complexes, the compiled results show that H_2O_2 significantly impairs mitochondrial function.

After the addition of P188, mitochondria were either placed back on ice immediately or, as presented above, kept at RT for further 10 min resulting in a total of 10 or 20 min exposure to RT (10 min RT; 20 min RT), respectively. The results of these different procedures were assessed through ATP synthesis and O_2 consumption (cf. 3.2 Comparison of Different Times of Exposure to Room Temperature on Isolated Mitochondria). ATP synthesis for both complex I and II substrates was significantly

lower after 20 min RT than after 10 min RT. In addition, when complex II substrate was given, no significant impairment of ATP synthesis by H_2O_2 after 20 min RT was observed in contrast to after 10 min RT. O_2 consumption data could not be statistically analyzed because of partially insufficient sample sizes (n=2); however, O_2 consumption for complex I substrates appeared to be much higher after only 10 min RT compared to 20 min RT (Figure 23). In conclusion, the results show that exposure to RT quickly reduced function of rat brain isolated mitochondria as assessed by ATP synthesis and O_2 consumption. Yet, the 20 min RT setting is a more accurate simulation of I/R injury than the 10 min RT setting as the latter does not provide a representation of reperfusion in form of the 10 min of RT after P188 addition.

In contrast to the in vitro H_2O_2-induced injury, an in vivo injuring approach was performed to account for in vivo processes during ischemia which may not be reproduced in vitro. Asphyxial cardiac arrest was induced in rats in vivo before isolating brain mitochondria and applying 250 or 500 µM P188. Here, mitochondrial function was assessed only through O_2 consumption.

For complex I substrates, 10 or 15 min of asphyxia significantly impaired O_2 consumption of isolated mitochondria continuously kept on ice compared to no asphyxia (sham) and no significant differences were found between 10 and 15 min of asphyxia. Exposure of mitochondria to RT for 10 min after isolation as done in control and P188-treated mitochondria further reduced O_2 consumption significantly, hereby concealing the differences that could be observed by asphyxia in mitochondria continuously kept on ice. Although O_2 consumption did not significantly decrease in control and P188-treated mitochondria under the 10 min asphyxia condition, the same trend was yet observable.

Finally, independently from the injury mechanism (except for a slight but significant decrease of ATP synthesis and O_2 consumption in the control+P188 group compared to only control when looking at the percentages of control in complex II) P188 did not show significant effects on mitochondria and was not able to alleviate mitochondrial impairment after simulation of I/R injury.

4.2 Methods of Injuring Isolated Mitochondria

P188's superb protective effects after I/R injury have been recreated in various experimental settings on both the heart and the brain [40–47,49,50,55,56,62]. Therefore, injuring mitochondria in a way that mimics the pathophysiological processes

of I/R in living cells was the premise to show any direct effects of P188 on mitochondria. The following chapters discuss different methods to indirectly or directly injure mitochondria in vivo, ex vivo, in vitro, and in vitro in cell cultures or isolated mitochondria.

4.2.1 In Vivo Injury

In the present study the induction of global and, specifically, cerebral ischemia by asphyxial cardiac arrest of 10 or 15 min in rats in vivo was thought to reflect a realistic injury. Brain mitochondria were isolated immediately after ischemia without yet introducing reperfusion. Only when isolated, mitochondria would then be exposed to RT and P188 at the same time to simulate reperfusion as P188 seems to work optimally when applied at the beginning of reperfusion [45]. By isolating mitochondria first before adding P188, it was ensured that no cellular processes could detract from P188's potential direct interaction with mitochondria.

While isolating mitochondria before introducing reperfusion seems to be an alternative approach the basic model of I/R in vivo and ex vivo has already been described in the literature for the brain as well as for the heart. In fact, in 2015 Kleinbongard et al. presented an in vivo mouse model in which 30 min of left anterior descending coronary artery (LAD) occlusion with subsequent 120 min of reperfusion were performed resulting in an infarct size of approximately 35% of the heart's area at risk [81]. Similarly, Yang et al. implemented LAD occlusion for 35 min followed by 120 min of reperfusion in an in vivo rat model which led to an infarct size of approximately 55% of the heart's area at risk [82]. In an in vivo pig model with 45 min of left coronary artery occlusion and subsequent 4 h of reperfusion Bartos et al. showed an infarct size of about 40% of the heart's area at risk [45]. These findings show the difficulty in discovering an appropriate amount of damage with potential for attenuation by protective strategies as well as for further damage, and the dependence on the animal species.

Looking at the brain instead of the heart, Luo et al. used 60 min of middle cerebral artery occlusion without any reperfusion in mice resulting in an infarct volume of approximately 60% of the ipsilateral hemisphere [55]. Given the much longer duration of ischemia compared to the time of asphyxia in the present study (10 or 15 min), the question arises if the brain and, consequently, brain mitochondria were damaged sufficiently in the present study. However, with only a slightly longer time of ischemia,

Yang et al. caused severely more damage in rat hearts than Kleinbongard et al. in mouse hearts [81,82]. Although these results were achieved in hearts instead of brains, they may perhaps be hinting that rats are more susceptible to ischemic damage than mice. This would explain how a significant decrease of O_2 consumption was observable after only 10 or 15 min of asphyxia, since in the present study, too, rats were used instead of mice.

Some studies went a step further and, as in the present study, analyzed mitochondrial function instead of infarct size after in vivo ischemia in both the heart and the brain. In the aforementioned study, Bartos et al. isolated pig heart mitochondria after 45 min ischemia and 4 h reperfusion and observed a drop in O_2 consumption from an RCI of 8 to 4 for complex I substrates and from 3.5 to 2.0 for complex II substrate [45]. This reduction of approximately 50% is slightly higher than the reduction of RCI in the present study; however, the ischemic time was three to four times as long [45]. Matsuura et al., too, used a pig model in which they examined the effects of global ischemia after ventricular fibrillation for 19 min or for 15 min with 4 min of reperfusion (cardiopulmonary resuscitation) [71]. Here, cardiac as well as cerebral mitochondria were examined: Compared to no ischemia, O_2 consumption of cardiac mitochondria was only significantly reduced for complex II substrate after ischemia both with and without reperfusion [71]. Interestingly, O_2 consumption of cerebral mitochondria was significantly reduced for both complex I and II substrates after ischemia and independently from reperfusion, showing the high susceptibility of brain mitochondria to ischemic damage [71]. In this case, the time of ischemia and the reduction of O_2 consumption approximately match the ones used and achieved in the present study [71]. However, this must be viewed with a caveat as these results were achieved in pigs and not in rats [45,71].

4.2.2 Ex Vivo Injury

I/R injury is often mimicked ex vivo, too. For example, Yang et al. presented an ex vivo model in a guinea pig isolated heart [82]. They blocked the aortic and coronary flow for 35 min and reperfused the heart thereafter for 120 min [82]. In a rat isolated heart Langendorff model [83], Makazan et al. induced global ischemia for 20 or 30 min by blocking the coronary flow and reperfused the heart for another 30 min before isolating the mitochondria; they were able to show that 30 min of ischemia significantly reduced mitochondrial O_2 consumption [84]. With 40 min ischemia and 30 min of reperfusion a

similar timeframe was chosen by Chen et al. for their mouse isolated heart model [85]. Chen, Lesnefsky and co-workers also used 30 min ischemia in a rabbit isolated heart model [85,86]. Interestingly, they did not use reperfusion in this model and instead proceeded directly to the isolation of mitochondria resulting in decreased CRC and mitochondrial bcl-2 – an anti-apoptotic protein – content [85,86].

Eskaf et al. applied ischemia of 30 min without and with 10 min of reperfusion in their Langendorff rat isolated heart model and here, interestingly, the outcome in later isolated mitochondria was not always the same: Compared to the respective time controls ATP synthesis decreased independently of reperfusion and for both complex I and II. However, O_2 consumption was only decreased when reperfusion was omitted. This was similar to the measured CRC which was only significantly decreased without reperfusion in complex II [87]. These differences in dependence of the assay were not completely conclusive and a trend was often observable even when non-significant [87].

While these ex vivo methods certainly have some benefits regarding the function of a certain organ during I/R, an in vivo setting is better suited to recreate the pathophysiology that actually occurs during I/R globally, thus asphyxial cardiac arrest was used as well in the present study to simulate global ischemia.

4.2.3 In Vitro Cell Culture Injury

Cell cultures as an in vitro experimental setting have also been used when simulating I/R injury, some even with the scope of injuring specifically mitochondria within the cells [81,88,89]. Sakamoto et al. applied mineral oil to isolate cardiac myocytes from air for either 30 or 120 min and isolated mitochondria thereafter to measure its Ca^{2+} flow [89,90]. However, the OGD is more commonly used [49,55,80,81]. In cardiomyocytes OGD for 60 min with 5 min of reoxygenation were performed by Kleinbongard et al. to then analyze ROS production from mitochondria [81]. However, OGD time spans vary from study to study. In fact, Ozcan et al. made H9c2 cardiomyocytes undergo 12 h of OGD followed by 12 h of reoxygenation before analyzing cell and mitochondrial morphology through electron microscopy [88]. Interestingly, they wanted to simulate only reperfusion without ischemia as well. To do that, H9c2 cardiomyocytes were injured with 100 µM H_2O_2 for 1 h which significantly impaired cellular and mitochondrial ultrastructure, although cell survival was not as strongly diminished compared to OGD with reoxygenation as a combined I/R injury [88]. Evidently, in vitro cell cultures are

effective at injuring mitochondria after simulated I/R injury. Nonetheless, isolated mitochondria are usually isolated from entire organs and not from cell cultures, making it not feasible to treat mitochondria from cell cultures directly with P188, thus making the injury of already isolated mitochondria the more appropriate approach.

4.2.4 In Vitro Isolated Mitochondria Injury

Injuring mitochondria after the isolation proves to be favored when trying to study their specific behavior in I/R injury, as it allows for more targeted alterations in mitochondrial processes. This becomes evident when looking at the vast literature on this topic [81,84–86,88,91–97]. For instance, anoxia/reoxygenation is an established method to simulate I/R injury in isolated mitochondria, similar to in vivo and ex vivo settings as well as in vitro cell cultures [81,88,92,95]. Ozcan et al. sealed rat isolated cardiac mitochondria in an airtight multichannel chamber letting the mitochondria consume the O_2 within 5 min to create anoxic conditions [95]. As soon as the O_2 was completely consumed, 20 min of anoxia were timed before exposing the mitochondria to RT for another 20 min [88,95]. This procedure led to a significantly decreased ATP synthesis and O_2 consumption [95]. Interestingly, the treatment of mitochondria with ROS scavengers significantly attenuated the anoxic damage, hinting to the detrimental effects of ROS on mitochondria that were shown in the present study as well [95]. In contrast to that, Korge et al. used a closed cuvette to conduct their rabbit isolated heart mitochondria experiments in. Instead of waiting for the mitochondria to consume the O_2 they actively directed nitrogen (N_2) into the buffer with the mitochondria through a hole in the cuvette cover [92]. To reoxygenate, they then simply exchanged the N_2 for O_2 [92]. Another study describes generating anoxia in mouse isolated heart mitochondria by introducing argon into the buffer until O_2 concentration decreased below <15 nmol O_2 ml^{-1} [81]. Anoxia was then maintained for 6 min before adding air-saturated incubation buffer to the mitochondria for another 3 min to simulate reperfusion, again, leading to decreased ATP synthesis, O_2 consumption and also CRC compared to a time control [81].

As described above (cf. 1.3 Ischemia/Reperfusion Injury), Ca^{2+} overload occurs during I/R and contributes to the opening of mPTPs [35,37,38]. By adding Ca^{2+} to isolated mitochondria, these circumstances can be replicated fairly easily [91,93,96]. For instance, Crestanello et al. added Ca^{2+} in concentrations of 0.1 or 0.5 µM to rat isolated heart mitochondria and were able to observe that increasing Ca^{2+} concentrations

uncoupled mitochondrial oxidative phosphorylation [91]. In a study focusing specifically on the role of complex II in the production of ROS, 50 µM of Ca^{2+} induced MPT as well as increased production of H_2O_2, and this was inhibited by pre-incubating the rabbit isolated cardiac mitochondria with EGTA to chelate Ca^{2+} [93]. Another study examining a radical scavenger to inhibit MPT found that addition of Ca^{2+} (30 to 300 µM) to rat isolated brain mitochondria caused an increased ROS production in a dose-dependent manner [96]. This shows that the same mechanism used in the present study to calculate the CRC, namely the activation of MPT through the addition of Ca^{2+}, can be used to simulate one particular aspect of I/R in mitochondria. Furthermore, it is interesting to observe that Ca^{2+} overload also contributes to ROS production as this could mean that Ca^{2+} overload happens more upstream in the reaction chain of I/R.

As mentioned above, bcl-2 acts anti-apoptotic by inhibiting pro-apoptotic proteins and its content in mitochondria has been shown to correlate with the state of the respiratory chain [86]. Furthermore, bcl-2 depletion seems to be conducive for the opening of mPTPs [86]. This can be utilized to, again, induce MPT by inhibiting bcl-2 which results in increased mitochondrial swelling and cytochrome c release as well as decreased CRC [85,86].

Lastly, ROS as a well-investigated component of I/R injury have been used to simulate the latter in isolated mitochondria [84,86,88,94,96,97]. This approach was used already in 1986 when Malis and Bonventre added hypoxanthine (25 µM), xanthine oxidase (0.3 U), and ferrous chloride (20 µM) to rat isolated renal mitochondria resulting in a decrease of mitochondrial respiration for both complex I and II substrates [94]. Interestingly, they also added Ca^{2+} at a concentration of 30 nmol mg^{-1} mitochondrial protein and, while this showed no impact on mitochondrial function by itself when combined with ROS, it significantly decreased mitochondrial respiration even further when complex I substrates were given compared to only ROS [94]. Similarly, Makazan et al. used xanthine (0.3 mM) and xanthine oxidase (11 mU) for 1, 2, or 3 min on rat isolated heart mitochondria resulting in reduced mitochondrial respiration in a time-dependent manner [84]. Although the amount of ROS produced was not quantified, these findings once more exemplify the harming effect of ROS on mitochondria which were again confirmed in the present study.

Instead of combining an enzyme and its substrate to create ROS, Makazan et al. also added H_2O_2 as a ROS itself to the mitochondria [84]. This was done for 3 min at concentrations of 10, 20, and 30 µM, again causing decreased mitochondrial

respiration, this time in a concentration-dependent manner [84]. H_2O_2 was also used in the aforementioned study of Ozcan et al. at a concentration of 100 µM for 30 min causing the rat isolated heart mitochondria to swell by approximately 33% [88]. When using concentrations between 10 and 300 µM, they were able to show that H_2O_2 inhibits ATP production in a concentration-dependent manner, with the strongest decrease being from 100 to 200 µM [88]. On their rabbit isolated heart mitochondria, Chen and Lesnefsky, too, used 100 µM of H_2O_2 but for only 5 min [86]. Still, they were able to observe significant mitochondrial swelling [86]. This could mean that H_2O_2 induced damage to isolated mitochondria is not time-dependent. However, H_2O_2 has been used at even higher concentrations, namely 2 mM H_2O_2 for 5 min in rat isolated cardiac mitochondria or 3 mM H_2O_2 for 7 min on rat isolated brain mitochondria [96,97]. For the present study, 200 µM H_2O_2 for 10 min as a setting for I/R simulation was chosen as it offered a significant decrease of mitochondrial function parameters with potential for the damage to be further exacerbated or, rather, ameliorated by other means.

4.3 Poloxamer 188 on Mitochondria

As mentioned previously (cf. 1.4 Poloxamer 188), Bartos et al. were able to show in a porcine model of myocardial infarction that, when applied directly upon reperfusion, P188 is able to not only decrease serum troponin I and infarct size but also to improve mitochondrial function assessed by mitochondrial respiration and Ca^{2+} retention [45]. These results led to the hypothesis that mitochondria might be directly affected by P188, and consequently to the present study. Bartos et al., however, were not the only ones that specifically examined mitochondrial function after treating animals or cell cultures with P188 [50,51,55,56,62,80,98,99].

In 2008, Kilinc et al. used chick forebrain neuron cultures to analyze the effects of 100 µM P188 after shear stress injury [50]. Shear stress injury simulates diffuse axonal injury as it occurs in TBI and resulted in axonal bead formation and cytoskeletal damage similar to diffuse axonal injury in vivo [50]. The bead formation was concurrent with the local decrease in microtubule content [50]. When staining mitochondria, it became apparent that they accumulate in the axonal beads [50]. P188, however, was able to significantly reduce axonal beading, thus supporting the hypothesis that P188 directly interferes with mitochondria [50]. In 2009, Kilinc et al. used the same approach but went a step further in analyzing the Ca^{2+} and calpain (a Ca^{2+}-activated protease)

response of the axon to the shear stress injury [51]. By doing so, they were able to show that axonal beading is most likely caused by calpain activation which was higher when Ca^{2+} was available and when the cell membrane was permeable [51]. Inversely, calpain activation could be blocked by chelating intra- or extracellular Ca^{2+} or by sealing the cell membrane with P188 [51]. In addition, calpain activity showed focal peaks that coincided with mitochondria accumulation and that would show axonal beads later on [51]. They, therefore, were able to predict the localization of axonal bead formation by taking into account focal calpain activity and mitochondrial distribution [51]. Again, this highlights the possibility that mitochondria play a major role in channeling P188's positive effects. In another study a combination of peak and steady shear stress was used to injure rat primary cortical neurons [56]. After shear stress injury, neurons were treated with P188 (50, 100, or 150 μM) for 6 or 24 h [56]. P188 attenuated cell death by shear stress injury and cell morphology changes [56]. In the context of mitochondria, P188 was able to temper loss of $\Delta\psi_m$ and release of cytochrome c from the mitochondria into the cytosol, both indicators of mitochondrial membrane permeabilization [56]. P188 furthermore decreased tBID (a pro-apoptotic protein that induces poration of outer mitochondrial membrane [62,100]) in mitochondria to levels of uninjured sham neurons [56]. This shows how closely P188's effects are intertwined with mitochondrial function further reinforcing potential direct effects of P188 on mitochondria.

While Kilinc et al.'s experiments focused on diffuse axonal injury as a part of TBI, they did not focus on I/R which can very well be simulated in cell cultures through OGD. Shelat et al. for instance used OGD for 30, 45, or 60 min with subsequent 48 h of reoxygenation on rat hippocampal neurons [80]. They then treated the cells with P188 in concentrations of 0.3, 3, 30, or 100 μM and for 1, 6, 12, 15, 18, or 24 h after OGD [80]. P188 was able to rescue hippocampal neurons from apoptosis after OGD, and this was done optimally at a concentration of 30 μM and up to 12 h after injury [80]. Shelat et al. were able to detect that P188 prevents a variety of detrimental intracellular processes such as caspase activation, mitochondrial cytochrome c release, loss of $\Delta\psi_m$ and inhibition of BAX (an effector protein that causes permeabilization of outer mitochondrial membrane) translocation from the cytoplasm to the mitochondria [80]. In another study by Luo et al., 18 h of OGD on mouse primary cortical neurons followed by reoxygenation overnight were chosen as the experimental setup [55]. In different assays, the neurons were treated with P188 at concentrations ranging between 0.1 nM

and 100 µM 10 min after OGD [55]. Using an LDH assay, Luo et al. were able to show that P188 was able to rescue the neurons from OGD-induced cell death starting at a concentration of 10 nM [55]. P188 furthermore inhibited loss of $\Delta\psi_m$ as well as release of cytochrome c and activation of caspase-3 [55]. These results prove to be highly concordant with Shelat et al.'s accentuating the potential for direct interaction of P188 with mitochondria [80]. In addition, in a study by Wang et al., embryonic rat hippocampal cells were exposed to 45 min of OGD followed by 2 h of reoxygenation and incubation with fluorescently labeled P188 [62]. Wang et al. were able to observe that P188 localizes to neuronal mitochondria but only in cells subjected to OGD [62].

Because of the previous studies reporting about the inhibition of loss of cytochrome c and $\Delta\psi_m$, as well as prevention of BAX translocation from the cytosol to mitochondria, Wang et al.'s study furthermore asked if P188 could inhibit poration of the outer mitochondrial membrane, specifically [62]. Incubation with 30 nM staurosporine for 24 h was used in mouse embryonic fibroblasts to induce poration of the outer mitochondrial membrane in a cellular model, and incubation with 1.5 nM tBID for 30 min was used to achieve the same in rat isolated brain mitochondria [62]. Fibroblasts or mitochondria were treated with P188 (1, 3, 10, 30, or 100 µM) throughout the 24 h or 30 min, respectively [62]. Mouse embryonic fibroblasts showed increased survival when treated with P188 in a dose-dependent matter with significantly improved survival at a minimum of 10 µM P188 and the highest survival at 100 µM P188 [62]. In rat isolated brain mitochondria, cytochrome c release was measured to assess P188's efficacy [62]. Here, cytochrome c release was significantly reduced in P188 treated mitochondria starting at a concentration of 10 µM [62]. The strongest reduction in cytochrome c release was seen at 30 µM P188, while 100 µM P188 only reduced cytochrome c release as strongly as 10 µM P188 [62].

The recent study by Eskaf et al. (cf. 4.2.2 Ex Vivo Injury) also applied P188 directly on isolated mitochondria [87]. After subjecting ex vivo rat isolated hearts to ischemia 1 mM P188 was applied either in a reperfusion period after ischemia and/or during the process of isolating mitochondria [87]. In contrast to the aforementioned studies P188 did not rescue mitochondrial function assessed by ATP synthesis, O_2 consumption, and CRC independently of the time of administration (during reperfusion and/or during isolation of mitochondria). The absence of an effect of P188 when applied ex vivo during reperfusion is particularly surprising as this has been proven effective in Bartos et al.'s study [45]. However, Eskaf et al. hypothesized that this is due to the reperfusion

period only amounting to 10 min [87]. When given during reperfusion as well as during mitochondria isolation P188 even showed a detrimental trend. In this case the authors suggested an exceedance of P188's critical micelle concentration causing the concentration of free and therefore active P188 to actually decrease rather than increase [87].

To date, Wang et al.'s study is the only one that has found direct rescuing effects of P188 on isolated mitochondria. However, the positive results of P188 on isolated mitochondria in their study stand in stark contrast to the non-existent effect of P188 shown in Eskaf et al.'s or the present study. There are, however, some pronounced differences in the methodical approach of these studies. One major distinction is the method of injuring isolated mitochondria: While in vivo ischemia or the ROS H_2O_2 used in the present study damage mitochondria at various sites [101], Wang et al. applied tBID to selectively induce poration only of the outer mitochondrial membrane [62]. Accordingly, Wang et al. measured cytochrome c release from mitochondria as this specifically depicts the state of the outer mitochondrial membrane [62]. However, poration of the outer mitochondrial membrane is only one particular component of I/R injury, in which P188 has now proven to be effective [35,62]. In contrast, injury of isolated mitochondria with ischemia in vivo or H_2O_2 in vitro represents a broader spectrum of I/R injury [35,101] and after injuring mitochondria this way P188 was not able to rescue mitochondrial function in the present study. This begs the question if the sole reduction of outer mitochondrial membrane poration seen in Wang et al.'s study can account for the highly improved mitochondrial function after P188 application in vivo, originally seen by Bartos et al. [45,62]. Another very interesting distinction to be made is the concentration in which P188 was applied: Wang et al. observed the greatest effect at 30 µM P188 and less effect at 100 µM [62]. In conjunction with the results of the present study, this could perhaps suggest that at a concentration of 250 µM or more P188 may be partly damaging to isolated mitochondria, therefore counteracting its own positive properties. While in this specific setting of asphyxia-induced cardiac arrest in vivo or H_2O_2-induced injury in vitro, no effects of P188 could be observed, these assumptions could lead the way to further experiments in which P188 is tested on isolated mitochondria at different concentrations and after different injury mechanisms.

4.4 Study Limitations

To properly review and discuss the results of the present study a few limitations have to be taken into consideration:

a) The data that resulted from the experiments made in the course of the present study show a great variance between different experiment days, which is the reason why the data was not only presented as absolute values but also as percentages of control. The reason for this variance is most likely due to progressive improvement in the execution of the experimental procedure, since mitochondrial function parameters typically rather increased from experiment day to experiment day. Although percentages of control were used to account for this, the statistical analysis of the absolute values was limited by the prevalence of high variance, possibly showing less significant differences than actually existed.

b) As shown previously (cf. 3.2 Comparison of Different Times of Exposure to Room Temperature on Isolated Mitochondria), rat isolated brain mitochondria reacted very sensibly to exposure to RT, making this alone a factor that can poorly be accounted for. The exposure to RT for only 10 more min significantly decreased ATP synthesis of isolated mitochondria. Similarly, in a study from Kleinbongard et al., isolated mitochondria showed lower mitochondrial respiration between a time control sample of mouse isolated heart mitochondria which was exposed to RT for 9 min and a baseline sample which was analyzed directly after isolation [81]. Yet, the exposure to RT is essential for the metabolic processes inside the mitochondria to occur and therefore to simulate reperfusion appropriately. While no further research has been found on this specific topic, the effect or RT shown on mitochondria may account for a confounding factor in a lot of studies of isolated mitochondria, including this one.

c) P188 did not preserve mitochondrial function after asphyxial cardiac arrest in vivo when given after the isolation of mitochondria. While this concurs with the results achieved in H_2O_2-injured mitochondria, it is not known how well the state of mitochondria is being preserved throughout the isolation process. Throughout the isolation process the mitochondrial sample is cooled down to 4°C to slow down metabolic processes inside it, however it is unclear if the ischemic damage – as a metabolic process itself – is actually “frozen” in the mitochondria. Therefore, a possible prolongation of ischemic damage inside the mitochondria could be an

explanation for why P188 did not alter mitochondrial function after asphyxial cardiac arrest in vivo.

d) Mitochondrial function was, as mentioned in a), dependent on the quality of execution of the experimental procedure which was mainly comprised of the isolation process. This, generally, begs the question how much mitochondria are impaired during the isolation process even if executed perfectly. Therefore, there is a possibility that mitochondria are injured during the isolation such that P188 cannot rescue them anymore.
e) As mentioned previously (cf. 4.2 Methods of Injuring Isolated Mitochondria), mitochondrial impairment by H_2O_2 occurs in a concentration-dependent manner [88]. It may very well be possible that, in the present study, mitochondria were simply injured too excessively and that a smaller concentration of H_2O_2 would have allowed for the injury to be attenuated by P188.
f) In the present study, P188 was only used on mitochondria at concentrations of or exceeding 250 µM following preliminary research in the Riess laboratory [102]. However, in Wang et al.'s study, the optimal concentration seemed to be at 30 µM [62]. Perhaps, the P188 is only able to attenuate impairment in isolated mitochondria at lower concentration as the ones tested in the present study.
g) Oftentimes, significant differences were not detected, although a clear trend was recognizable. This may be due to the relatively small sample sizes used in the present study. A study needs a sufficient sample size to effectively reduce the possibility that differences mistakenly remain undetected. The likelihood that such a mistake has not been done is defined as power [103]. As the mitochondrial yield from one animal was very low, only few data points could be extracted from using one animal. This made the experiments of this study very resource-intensive and the limited number of animals (total of 43) caused the sample size to be restricted to a small number, potentially decreasing the present study's power. In turn, trends observable in the present study, may be of greater interest, as a larger sample size and consecutively greater power may have disclosed more significant differences.

4.5 Future Directions

In retrospective, the present study was not able to show any effects of P188 at concentrations of 250 or 500 µM on rat isolated brain mitochondria after simulated I/R injury in vivo or in vitro. From the literature review, however, it becomes apparent that

there are many variables to be considered when evaluating these results. Consequentially, future studies should investigate these variables, the first one being the type of injury to the mitochondria:

While isolated mitochondria showed functional impairment after both in vivo and in vitro injury, neither of these injuries were attenuated by P188. As mentioned above (cf. 4.6 Study Limitations) it is not known how well the mitochondrial state is preserved during isolation after ischemic injury; therefore, it could be considered varying the time span between end of ischemic injury in vivo and P188 treatment after isolation in vitro to appraise the extent of this variable. In regard to the in vitro injury, using smaller concentrations of H_2O_2 before P188 treatment could clear the question if mitochondria were injured too extremely. Furthermore, different injury methods such as anoxia/reoxygenation or Ca^{2+} overload could prove to be more sensible to P188 treatment (cf. 4.2 Methods of Injuring Isolated Mitochondria) [81,88,91–96].

After discussing potential alternatives to the injury methods used in the present study, the method of treatment as the remaining variable could be modified, too:

For one, Wang et al.'s study displays the importance of finding a concentration optimum for P188 (cf. 4.6 Study Limitations) [62]. The treatment of mitochondria after simulated I/R injury with different concentrations of P188 is, therefore, of major interest for the future. Concentrations of P188 as used in Wang et al.'s study could also yield protective effects in mitochondria injured as in the present study [62]. Hereby, the injury model used in the present study would yet appear suitable to reveal protective effects of P188.

Furthermore, the importance of the ratio between the hydrophobic PPO and the hydrophilic PEO within block copolymers has recently become more apparent [41]. As the ratio between PPO and PEO dictates the hydrophobicity of triblock copolymers such as P188 (cf. 1.4.1 Chemical Properties and Principal of Biological Effects), potential alternatives to P188 are being discovered in the form of diblock copolymers [41]. These types of block copolymers which only have one PEO side chain attached to the hydrophobic PPO center leave the option to alter the other end of the hydrophobic PPO synthetically, thereby diminishing or increasing its hydrophobicity [41]. This may prove to be more effective than P188 in rescuing cells and perhaps even mitochondria after I/R injury.

Taken together, it is far too early to draw a conclusion if P188's protective effects on cells and organisms are achieved by acting directly on mitochondria. As described

above, both the injury and the treatment of isolated mitochondria shown in the present study can be modulated to discover a more complete picture of how P188 interacts with mitochondria.

5 Summary

To this day, the patient's outcome after any form of cerebral ischemia is often mediocre at best. The added damage that occurs at reperfusion after ischemia seems to be as important as the ischemic injury itself. New therapeutic strategies targeted at this critical issue are therefore crucial. P188, an amphiphilic triblock copolymer, has risen to be one of the most promising pharmacological therapeutics, as its capability to insert into injured cell membranes seems to perfectly fit the needed criteria to protect against I/R injury. Lately, it has become apparent that mitochondrial function particularly profits from P188 treatment after I/R injury. Therefore, the question arose, if P188 may interact directly with mitochondria.

In the present study, rat isolated brain mitochondria were injured and then treated with P188. The injury took place either in vivo by asphyxial cardiac arrest before isolation of mitochondria or in vitro after isolation by addition of the ROS H_2O_2. After treatment with P188, mitochondrial function was evaluated through the assessment of ATP synthesis, O_2 consumption and CRC.

10 or 15 min of asphyxia in vivo as well as 200 µM H_2O_2 for 10 min in vitro significantly impaired mitochondrial function. Furthermore, a damaging effect of RT on isolated mitochondria became apparent. Contrary to the underlying hypothesis, P188 did not preserve mitochondrial function independently of the injury mechanism chosen.

In conclusion, in the context of studying P188, two new methods of I/R injury simulation, namely asphyxial cardiac arrest in vivo and the injury with H_2O_2 in isolated mitochondria in vitro, have been established. However, it is not yet conclusive, if P188 does or does not directly improve mitochondrial function after I/R injury. Further research looking at different injuring methods as well as modulating the treatment method is needed to ultimately clarify this question.

6 References

1. Feigin, V. L.; Norrving, B.; Mensah, G. A. Global Burden of Stroke. *Circ Res* **2017**, *120*, 439-448.
2. Hankey, G. J. Stroke. *Lancet* **2017**, *389*, 641-654.
3. Heuschmann, P. U.; Busse, O.; Wagner, M.; Endres, M.; Villringer, A.; Röther, J.; Kolominsky-Rabas, P. L.; Berger, K. Schlaganfallhäufigkeit und Versorgung von Schlaganfallpatienten in Deutschland. *Aktuelle Neurologie* **2010**, *37*, 333-340.
4. Statistisches Bundesamt (Destatis). Gestorbene: Deutschland, Jahre, Todesursachen. Available online: https://www.destatis.de (accessed on 5. Aug, 2021).
5. Stroke Unit Trialists' Collaboration. Organised inpatient (stroke unit) care for stroke. *Cochrane Database Syst Rev* **2013**, CD000197.
6. Yokobori, S.; Nakae, R.; Yokota, H.; Spurlock, M. S.; Mondello, S.; Gajavelli, S.; Bullock, R. M. Subdural hematoma decompression model: A model of traumatic brain injury with ischemic-reperfusional pathophysiology: A review of the literature. *Behav Brain Res* **2018**, *340*, 23-28.
7. Hackenberg, K.; Unterberg, A. [Traumatic brain injury]. *Nervenarzt* **2016**, *87*, 203-14; quiz 215.
8. Sinha, N.; Parnia, S. Monitoring the Brain After Cardiac Arrest: a New Era. *Current Neurology and Neuroscience Reports* **2017**, *17*.
9. Elmer, J.; Callaway, C. W. The Brain after Cardiac Arrest. *Semin Neurol* **2017**, *37*, 19-24.
10. Meschia, J. F.; Brott, T. Ischaemic stroke. *Eur J Neurol* **2018**, *25*, 35-40.
11. Sacco, R. L.; Kasner, S. E.; Broderick, J. P.; Caplan, L. R.; Connors, J. J.; Culebras, A.; Elkind, M. S.; George, M. G.; Hamdan, A. D.; Higashida, R. T.; Hoh, B. L.; Janis, L. S.; Kase, C. S.; Kleindorfer, D. O.; Lee, J. M.; Moseley, M. E.; Peterson, E. D.; Turan, T. N.; Valderrama, A. L.; Vinters, H. V.; American Heart Association Stroke Council, Council on Cardiovascular Surgery and Anesthesia; Council on Cardiovascular Radiology and Intervention; Council on Cardiovascular and Stroke Nursing; Council on Epidemiology and Prevention; Council on Peripheral Vascular Disease; Council on Nutrition, Physical Activity and Metabolism. An updated definition of stroke for the 21st century: a

statement for healthcare professionals from the American Heart Association/American Stroke Association. *Stroke* **2013**, *44*, 2064-2089.

12. Wilkinson, D. A.; Pandey, A. S.; Thompson, B. G.; Keep, R. F.; Hua, Y.; Xi, G. Injury mechanisms in acute intracerebral hemorrhage. *Neuropharmacology* **2018**, *134*, 240-248.
13. Foreman, P. M.; Harrigan, M. R. Blunt Traumatic Extracranial Cerebrovascular Injury and Ischemic Stroke. *Cerebrovasc Dis Extra* **2017**, *7*, 72-83.
14. Myerburg, R. J. Sudden cardiac death: exploring the limits of our knowledge. *J Cardiovasc Electrophysiol* **2001**, *12*, 369-381.
15. Sekhon, M. S.; Ainslie, P. N.; Griesdale, D. E. Clinical pathophysiology of hypoxic ischemic brain injury after cardiac arrest: a “two-hit” model. *Crit Care* **2017**, *21*, 90.
16. Yew, K. S.; Cheng, E. M. Diagnosis of acute stroke. *Am Fam Physician* **2015**, *91*, 528-536.
17. Diener, H.-C. *Leitlinien für Diagnostik und Therapie in der Neurologie*, 5th ed.; 2012; 1190
18. Powers, W. J.; Rabinstein, A. A.; Ackerson, T.; Adeoye, O. M.; Bambakidis, N. C.; Becker, K.; Biller, J.; Brown, M.; Demaerschalk, B. M.; Hoh, B.; Jauch, E. C.; Kidwell, C. S.; Leslie-Mazwi, T. M.; Ovbiagele, B.; Scott, P. A.; Sheth, K. N.; Southerland, A. M.; Summers, D. V.; Tirschwell, D. L. Guidelines for the Early Management of Patients With Acute Ischemic Stroke: 2019 Update to the 2018 Guidelines for the Early Management of Acute Ischemic Stroke: A Guideline for Healthcare Professionals From the American Heart Association/American Stroke Association. *Stroke* **2019**, *50*, e344-e418.
19. Turc, G.; Bhogal, P.; Fischer, U.; Khatri, P.; Lobotesis, K.; Mazighi, M.; Schellinger, P. D.; Toni, D.; de Vries, J.; White, P.; Fiehler, J. European Stroke Organisation (ESO) - European Society for Minimally Invasive Neurological Therapy (ESMINT) Guidelines on Mechanical Thrombectomy in Acute Ischaemic Stroke Endorsed by Stroke Alliance for Europe (SAFE). *Eur Stroke J* **2019**, *4*, 6-12.
20. Patil, K. D.; Halperin, H. R.; Becker, L. B. Cardiac arrest: resuscitation and reperfusion. *Circ Res* **2015**, *116*, 2041-2049.
21. Kleinman, M. E.; Brennan, E. E.; Goldberger, Z. D.; Swor, R. A.; Terry, M.; Bobrow, B. J.; Gazmuri, R. J.; Travers, A. H.; Rea, T. Part 5: Adult Basic Life

Support and Cardiopulmonary Resuscitation Quality: 2015 American Heart Association Guidelines Update for Cardiopulmonary Resuscitation and Emergency Cardiovascular Care. *Circulation* **2015**, *132*, S414-35.

22. Link, M. S.; Berkow, L. C.; Kudenchuk, P. J.; Halperin, H. R.; Hess, E. P.; Moitra, V. K.; Neumar, R. W.; O'Neil, B. J.; Paxton, J. H.; Silvers, S. M.; White, R. D.; Yannopoulos, D.; Donnino, M. W. Part 7: Adult Advanced Cardiovascular Life Support: 2015 American Heart Association Guidelines Update for Cardiopulmonary Resuscitation and Emergency Cardiovascular Care. *Circulation* **2015**, *132*, S444-64.
23. Perkins, G. D.; Handley, A. J.; Koster, R. W.; Castrén, M.; Smyth, M. A.; Olasveengen, T.; Monsieurs, K. G.; Raffay, V.; Gräsner, J. T.; Wenzel, V.; Ristagno, G.; Soar, J.; Adult, B. L. S. A. A. E. D. S. C. European Resuscitation Council Guidelines for Resuscitation 2015: Section 2. Adult basic life support and automated external defibrillation. *Resuscitation* **2015**, *95*, 81-99.
24. Soar, J.; Nolan, J. P.; Böttiger, B. W.; Perkins, G. D.; Lott, C.; Carli, P.; Pellis, T.; Sandroni, C.; Skrifvars, M. B.; Smith, G. B.; Sunde, K.; Deakin, C. D.; Adult, A. L. S. S. C. European Resuscitation Council Guidelines for Resuscitation 2015: Section 3. Adult advanced life support. *Resuscitation* **2015**, *95*, 100-147.
25. van der Bliek, A. M.; Sedensky, M. M.; Morgan, P. G. Cell Biology of the Mitochondrion. *Genetics* **2017**, *207*, 843-871.
26. Picard, M.; Wallace, D. C.; Burelle, Y. The rise of mitochondria in medicine. *Mitochondrion* **2016**, *30*, 105-116.
27. Nunnari, J.; Suomalainen, A. Mitochondria: in sickness and in health. *Cell* **2012**, *148*, 1145-1159.
28. Murphy, A. N.; Fiskum, G.; Beal, M. F. Mitochondria in neurodegeneration: bioenergetic function in cell life and death. *J Cereb Blood Flow Metab* **1999**, *19*, 231-245.
29. Alberts, B. *Molecular Biology of the Cell*, 6th ed.; Garland Science: 2017;
30. Horvath, S. E.; Rampelt, H.; Oeljeklaus, S.; Warscheid, B.; van der Laan, M.; Pfanner, N. Role of membrane contact sites in protein import into mitochondria. *Protein Sci* **2015**, *24*, 277-297.
31. Solaini, G.; Baracca, A.; Lenaz, G.; Sgarbi, G. Hypoxia and mitochondrial oxidative metabolism. *Biochim Biophys Acta* **2010**, *1797*, 1171-1177.

32. Zorova, L. D.; Popkov, V. A.; Plotnikov, E. Y.; Silachev, D. N.; Pevzner, I. B.; Jankauskas, S. S.; Babenko, V. A.; Zorov, S. D.; Balakireva, A. V.; Juhaszova, M.; Sollott, S. J.; Zorov, D. B. Mitochondrial membrane potential. *Analytical Biochemistry* **2018**, *552*, 50-59.
33. Kühlbrandt, W. Structure and function of mitochondrial membrane protein complexes. *BMC Biol* **2015**, *13*, 89.
34. Heinrich, P. C.; Müller, M.; Graeve, L. *Löffler/Petrides Biochemie und Pathobiochemie*, 9th ed.; Springer-Verlag: 2014; 1073
35. Kalogeris, T.; Baines, C. P.; Krenz, M.; Korthuis, R. J. Cell biology of ischemia/reperfusion injury. *Int Rev Cell Mol Biol* **2012**, *298*, 229-317.
36. Madathil, R. J.; Hira, R. S.; Stoeckl, M.; Sterz, F.; Elrod, J. B.; Nichol, G. Ischemia reperfusion injury as a modifiable therapeutic target for cardioprotection or neuroprotection in patients undergoing cardiopulmonary resuscitation. *Resuscitation* **2016**, *105*, 85-91.
37. Li, J.; Ma, X.; Yu, W.; Lou, Z.; Mu, D.; Wang, Y.; Shen, B.; Qi, S. Reperfusion promotes mitochondrial dysfunction following focal cerebral ischemia in rats. *PLoS One* **2012**, *7*, e46498.
38. Kristián, T.; Siesjö, B. K. Calcium in ischemic cell death. *Stroke* **1998**, *29*, 705-718.
39. Baines, C. P. The mitochondrial permeability transition pore and ischemia-reperfusion injury. *Basic Research in Cardiology* **2009**, *104*, 181-188.
40. Moloughney, J. G.; Weisleder, N. Poloxamer 188 (p188) as a membrane resealing reagent in biomedical applications. *Recent Pat Biotechnol* **2012**, *6*, 200-211.
41. Houang, E. M.; Bartos, J.; Hackel, B. J.; Lodge, T. P.; Yannopoulos, D.; Bates, F. S.; Metzger, J. M. Cardiac Muscle Membrane Stabilization in Myocardial Reperfusion Injury. *JACC Basic Transl Sci* **2019**, *4*, 275-287.
42. Poellmann, M. J.; Lee, R. C. Repair and Regeneration of the Wounded Cell Membrane. *Regenerative Engineering and Translational Medicine* **2017**, *3*, 111-132.
43. Marks, J. D.; Pan, C. Y.; Bushell, T.; Cromie, W.; Lee, R. C. Amphiphilic, tri-block copolymers provide potent membrane-targeted neuroprotection. *FASEB J* **2001**, *15*, 1107-1109.

44. Houang, E. M.; Sham, Y. Y.; Bates, F. S.; Metzger, J. M. Muscle membrane integrity in Duchenne muscular dystrophy: recent advances in copolymer-based muscle membrane stabilizers. *Skelet Muscle* **2018**, *8*, 31.
45. Bartos, J. A.; Matsuura, T. R.; Tsangaris, A.; Olson, M.; McKnite, S. H.; Rees, J. N.; Haman, K.; Shekar, K. C.; Riess, M. L.; Bates, F. S.; Metzger, J. M.; Yannopoulos, D. Intracoronary Poloxamer 188 Prevents Reperfusion Injury in a Porcine Model of ST-Segment Elevation Myocardial Infarction. *JACC Basic Transl Sci* **2016**, *1*, 224-234.
46. Justicz, A. G.; Farnsworth, W. V.; Soberman, M. S.; Tuvlin, M. B.; Bonner, G. D.; Hunter, R. L.; Martino-Saltzman, D.; Sink, J. D.; Austin, G. E. Reduction of myocardial infarct size by poloxamer 188 and mannitol in a canine model. *Am Heart J* **1991**, *122*, 671-680.
47. Effects of RheothRx on mortality, morbidity, left ventricular function, and infarct size in patients with acute myocardial infarction. Collaborative Organization for RheothRx Evaluation (CORE). [Abstract]. *Circulation* **1997**, *96*, 192-201.
48. Dong, H.; Qin, Y.; Huang, Y.; Ji, D.; Wu, F. Poloxamer 188 rescues MPTP-induced lysosomal membrane integrity impairment in cellular and mouse models of Parkinson's disease. *Neurochem Int* **2019**, *126*, 178-186.
49. Gu, J. H.; Ge, J. B.; Li, M.; Xu, H. D.; Wu, F.; Qin, Z. H. Poloxamer 188 protects neurons against ischemia/reperfusion injury through preserving integrity of cell membranes and blood brain barrier. *PLoS One* **2013**, *8*, e61641.
50. Kilinc, D.; Gallo, G.; Barbee, K. A. Mechanically-induced membrane poration causes axonal beading and localized cytoskeletal damage. *Exp Neurol* **2008**, *212*, 422-430.
51. Kilinc, D.; Gallo, G.; Barbee, K. A. Mechanical membrane injury induces axonal beading through localized activation of calpain. *Exp Neurol* **2009**, *219*, 553-561.
52. Meyer, L. J.; Salzman, M. M.; Eskaf, J.; Li, Z.; ML, R. Traumatic Brain Injury Simulation in a Mouse Neuronal Cell Culture Model [Abstract; accepted for WCA 2021]. **2020**.
53. Riess, M. L.; Meyer, L. J.; Eskaf, J.; Salzman, M. M.; Li, Z. Simulated Traumatic Brain Injury in Mouse Isolated Neurons is not Attenuated by Poloxamer 188 Postconditioning [Abstract; accepted for ASA 2020]. **2020**.
54. Lotze, F. P.; Salzman, M. M.; Pille, J. A.; Balzer, C.; Hees, J. E.; Cleveland, W. J.; Riess, M. L. Poloxamer 188 Protects Mouse Brain Microvascular Endothelial

Cells in an in-vitro Traumatic Brain Injury Model [Abstract]. *Circulation* **2019**, *140*, A22.

55. Luo, C.; Li, Q.; Gao, Y.; Shen, X.; Ma, L.; Wu, Q.; Wang, Z.; Zhang, M.; Zhao, Z.; Chen, X.; Tao, L. Poloxamer 188 Attenuates Cerebral Hypoxia/Ischemia Injury in Parallel with Preventing Mitochondrial Membrane Permeabilization and Autophagic Activation. *J Mol Neurosci* **2015**, *56*, 988-998.
56. Luo, C. L.; Chen, X. P.; Li, L. L.; Li, Q. Q.; Li, B. X.; Xue, A. M.; Xu, H. F.; Dai, D. K.; Shen, Y. W.; Tao, L. Y.; Zhao, Z. Q. Poloxamer 188 attenuates in vitro traumatic brain injury-induced mitochondrial and lysosomal membrane permeabilization damage in cultured primary neurons. *J Neurotrauma* **2013**, *30*, 597-607.
57. Moore, J. C.; Bartos, J. A.; Matsuura, T. R.; Yannopoulos, D. The future is now: neuroprotection during cardiopulmonary resuscitation. *Curr Opin Crit Care* **2017**, *23*, 215-222.
58. Pille, J. A.; Salzman, M. M.; Sonju, A. A.; Lotze, F. P.; Hees, J. E.; Cleveland, W. J.; Balzer, C.; Riess, M. L. Effect of Poloxamer 188 on Rat Brain Isolated Mitochondria After Exposure to Hydrogen Peroxide [Abstract]. *Circulation* **2019**, *140*, A355.
59. Wang, C.; Huang, R.; Li, C.; Lu, M.; Emanuele, M.; Zhang, Z. G.; Chopp, M.; Zhang, L. Vepoloxamer Enhances Fibrinolysis of tPA (Tissue-Type Plasminogen Activator) on Acute Ischemic Stroke. *Stroke* **2019**, *50*, 3600-3608.
60. Cadichon, S. B.; Le Hoang, M.; Wright, D. A.; Curry, D. J.; Kang, U.; Frim, D. M. Neuroprotective effect of the surfactant poloxamer 188 in a model of intracranial hemorrhage in rats. *J Neurosurg* **2007**, *106*, 36-40.
61. Colbassani, H. J.; Barrow, D. L.; Sweeney, K. M.; Bakay, R. A.; Check, I. J.; Hunter, R. L. Modification of acute focal ischemia in rabbits by poloxamer 188. *Stroke* **1989**, *20*, 1241-1246.
62. Wang, J. C.; Bindokas, V. P.; Skinner, M.; Emrick, T.; Marks, J. D. Mitochondrial mechanisms of neuronal rescue by F-68, a hydrophilic Pluronic block co-polymer, following acute substrate deprivation. *Neurochem Int* **2017**, *109*, 126-140.
63. Lamoureux, L.; Radhakrishnan, J.; Gazmuri, R. J. A Rat Model of Ventricular Fibrillation and Resuscitation by Conventional Closed-chest Technique. *J Vis Exp* **2015**.

64. Kristian, T. Isolation of mitochondria from the CNS. *Curr Protoc Neurosci* **2010**, *Chapter 7*, Unit 7.22.
65. Holmuhamedov, E. L.; Wang, L.; Terzic, A. ATP-sensitive K^+ channel openers prevent Ca^{2+} overload in rat cardiac mitochondria. *J Physiol* **1999**, *519 Pt 2*, 347-360.
66. Bradford, M. M. A rapid and sensitive method for the quantitation of microgram quantities of protein utilizing the principle of protein-dye binding. *Anal Biochem* **1976**, *72*, 248-254.
67. Salzman, M. M.; Riess, M. L. Personal communication. **2018**.
68. Katz, L.; Ebmeyer, U.; Safar, P.; Radovsky, A.; Neumar, R. Outcome model of asphyxial cardiac arrest in rats. *J Cereb Blood Flow Metab* **1995**, *15*, 1032-1039.
69. Riess, M. L.; Camara, A. K.; Heinen, A.; Eells, J. T.; Henry, M. M.; Stowe, D. F. K_{ATP} channel openers have opposite effects on mitochondrial respiration under different energetic conditions. *J Cardiovasc Pharmacol* **2008**, *51*, 483-491.
70. Riess, M. L.; Matsuura, T. R.; Bartos, J. A.; Bienengraeber, M.; Aldakkak, M.; McKnite, S. H.; Rees, J. N.; Aufderheide, T. P.; Sarraf, M.; Neumar, R. W.; Yannopoulos, D. Anaesthetic Postconditioning at the Initiation of CPR Improves Myocardial and Mitochondrial Function in a Pig Model of Prolonged Untreated Ventricular Fibrillation. *Resuscitation* **2014**, *85*, 1745-1751.
71. Matsuura, T. R.; Bartos, J. A.; Tsangaris, A.; Shekar, K. C.; Olson, M. D.; Riess, M. L.; Bienengraeber, M.; Aufderheide, T. P.; Neumar, R. W.; Rees, J. N.; McKnite, S. H.; Dikalova, A. E.; Dikalov, S. I.; Douglas, H. F.; Yannopoulos, D. Early Effects of Prolonged Cardiac Arrest and Ischemic Postconditioning during Cardiopulmonary Resuscitation on Cardiac and Brain Mitochondrial Function in Pigs. *Resuscitation* **2017**, *116*, 8-15.
72. Strathkelvin Instruments Limited. 1302 Microcathode Oxygen Electrodes. Available online: http://www.strathkelvin.com/wp-content/uploads/2015/04/electrode-manual.pdf (accessed on 13. Apr, 2020).
73. Strathkelvin Instruments Limited. Mitocell: Instructions for Use. Available online: http://www.strathkelvin.com/wp-content/uploads/2015/04/mt200-mt200A-manual.pdf (accessed on 13. Apr, 2020).
74. R Core Team. R: A language and environment for statistical computing. Available online: https://www.R-project.org/ (accessed on 29. Dec, 2020).

75. Fox, J.; Weisberg, S. *An {R} Companion to Applied Regression*, 3rd ed.; Sage: Thousand Oaks, CA, 2019;
76. Wickham, H.; François, R.; Henry, L.; Müller, K. dplyr: A Grammar of Data Manipulation. Available online: https://CRAN.R-project.org/package=dplyr (accessed on 29. Dec, 2020).
77. Kassambara, A. ggpubr: 'ggplot2' Based Publication Ready Plots. Available online: https://CRAN.R-project.org/package=ggpubr (accessed on 29. Dec, 2020).
78. de Mendiburu, F. agricolae: Statistical Procedures for Agricultural Research. Available online: https://CRAN.R-project.org/package=agricolae (accessed on 29. Dec, 2020).
79. Peters, G.-J. Y. userfriendlyscience: Quantitative analysis made accessible. Available online: https://userfriendlyscience.com (accessed on 29. Dec, 2020).
80. Shelat, P. B.; Plant, L. D.; Wang, J. C.; Lee, E.; Marks, J. D. The membrane-active tri-block copolymer pluronic F-68 profoundly rescues rat hippocampal neurons from oxygen-glucose deprivation-induced death through early inhibition of apoptosis. *J Neurosci* **2013**, *33*, 12287-12299.
81. Kleinbongard, P.; Gedik, N.; Witting, P.; Freedman, B.; Klöcker, N.; Heusch, G. Pleiotropic, heart rate-independent cardioprotection by ivabradine. *Br J Pharmacol* **2015**, *172*, 4380-4390.
82. Yang, M.; Camara, A. K. S.; Aldakkak, M.; Kwok, W. M.; Stowe, D. F. Identity and function of a cardiac mitochondrial small conductance Ca^{2+}-activated K^{+} channel splice variant. *Biochim Biophys Acta Bioenerg* **2017**, *1858*, 442-458.
83. Langendorff, O. Untersuchungen am überlebenden Säugethierherzen. *Archiv für die gesamte Physiologie des Menschen und der Tiere* **1895**, *61*, 291-332.
84. Makazan, Z.; Saini, H. K.; Dhalla, N. S. Role of oxidative stress in alterations of mitochondrial function in ischemic-reperfused hearts. *Am J Physiol Heart Circ Physiol* **2007**, *292*, H1986-94.
85. Chen, Q.; Xu, H.; Xu, A.; Ross, T.; Bowler, E.; Hu, Y.; Lesnefsky, E. J. Inhibition of Bcl-2 sensitizes mitochondrial permeability transition pore (MPTP) opening in ischemia-damaged mitochondria. *PLoS One* **2015**, *10*, e0118834.
86. Chen, Q.; Lesnefsky, E. J. Blockade of electron transport during ischemia preserves bcl-2 and inhibits opening of the mitochondrial permeability transition pore. *FEBS Lett* **2011**, *585*, 921-926.

87. Eskaf, J.; Cleveland, W. J.; Riess, M. L. No Direct Postconditioning Effect of Poloxamer 188 on Mitochondrial Function after Ischemia Reperfusion Injury in Rat Isolated Hearts. *Int. J. Mol. Sci.* **2021**, *22*.
88. Ozcan, C.; Terzic, A.; Bienengraeber, M. Effective pharmacotherapy against oxidative injury: alternative utility of an ATP-sensitive potassium channel opener. *J Cardiovasc Pharmacol* **2007**, *50*, 411-418.
89. Sakamoto, K.; Ohya, S.; Muraki, K.; Imaizumi, Y. A novel opener of large-conductance Ca^{2+} -activated K^+ (BK) channel reduces ischemic injury in rat cardiac myocytes by activating mitochondrial K_{Ca} channel. *J Pharmacol Sci* **2008**, *108*, 135-139.
90. Ohya, S.; Kuwata, Y.; Sakamoto, K.; Muraki, K.; Imaizumi, Y. Cardioprotective effects of estradiol include the activation of large-conductance Ca^{2+}-activated K^+ channels in cardiac mitochondria. *Am J Physiol Heart Circ Physiol* **2005**, *289*, H1635-42.
91. Crestanello, J. A.; Doliba, N. M.; Babsky, A. M.; Doliba, N. M.; Niibori, K.; Osbakken, M. D.; Whitman, G. J. Opening of potassium channels protects mitochondrial function from calcium overload. *J Surg Res* **2000**, *94*, 116-123.
92. Korge, P.; Honda, H. M.; Weiss, J. N. Protection of cardiac mitochondria by diazoxide and protein kinase C: implications for ischemic preconditioning. *Proc Natl Acad Sci U S A* **2002**, *99*, 3312-3317.
93. Korge, P.; John, S. A.; Calmettes, G.; Weiss, J. N. Reactive oxygen species production induced by pore opening in cardiac mitochondria: The role of complex II. *J Biol Chem* **2017**, *292*, 9896-9905.
94. Malis, C. D.; Bonventre, J. V. Mechanism of calcium potentiation of oxygen free radical injury to renal mitochondria. A model for post-ischemic and toxic mitochondrial damage. *J Biol Chem* **1986**, *261*, 14201-14208.
95. Ozcan, C.; Bienengraeber, M.; Dzeja, P. P.; Terzic, A. Potassium channel openers protect cardiac mitochondria by attenuating oxidant stress at reoxygenation. *Am J Physiol Heart Circ Physiol* **2002**, *282*, H531-9.
96. Takayasu, Y.; Nakaki, J.; Kawasaki, T.; Koda, K.; Ago, Y.; Baba, A.; Matsuda, T. Edaravone, a radical scavenger, inhibits mitochondrial permeability transition pore in rat brain. *J Pharmacol Sci* **2007**, *103*, 434-437.
97. Thummasorn, S.; Shinlapawittayatorn, K.; Khamseekaew, J.; Jaiwongkam, T.; Chattipakorn, S. C.; Chattipakorn, N. Humanin directly protects cardiac

mitochondria against dysfunction initiated by oxidative stress by decreasing complex I activity. *Mitochondrion* **2018**, *38*, 31-40.

98. Kirillova, G. P.; Mokhova, E. N.; Dedukhova, V. I.; Tarakanova, A. N.; Ivanova, V. P.; Efremova, N. V.; Topchieva, I. N. The influence of pluronics and their conjugates with proteins on the rate of oxygen consumption by liver mitochondria and thymus lymphocytes. *Biotechnol Appl Biochem* **1993**, *18*, 329-339.
99. Rapoport, N.; Marin, A. P.; Timoshin, A. A. Effect of a polymeric surfactant on electron transport in HL-60 cells. *Arch Biochem Biophys* **2000**, *384*, 100-108.
100. Esposti, M. D. The roles of Bid. *Apoptosis* **2002**, *7*, 433-440.
101. Sinha, K.; Das, J.; Pal, P. B.; Sil, P. C. Oxidative stress: the mitochondria-dependent and mitochondria-independent pathways of apoptosis. *Arch Toxicol* **2013**, *87*, 1157-1180.
102. William, K. S.; Salzman, M. M.; Douglas, H. F.; Balzer, C.; Shekar, K. C.; Riess, M. L. Copolymer Treatment Preserves Function of Isolated Cardiac Mitochondria Only When Given Immediately Upon Reperfusion. *Circulation* **2017**, *136*, A19445-A19445.
103. Sedgwick, P. The importance of statistical power. *BMJ* **2013**, *347*.

7 Appendix

7.1 Statuary Declaration

Hiermit erkläre ich, dass ich die vorliegende Dissertation selbständig verfasst und keine anderen als die angegebenen Hilfsmittel benutzt habe.

Die Dissertation ist bisher keiner anderen Fakultät, keiner anderen wissenschaftlichen Einrichtung vorgelegt worden.

Ich erkläre, dass ich bisher kein Promotionsverfahren erfolglos beendet habe und dass eine Aberkennung eines bereits erworbenen Doktorgrades nicht vorliegt.

Datum

Johannes Pille